Photovoltaic Maximum Power Point Tracker with Zero Oscillation and Adaptive Step

by

Francisco Paz

Ing., Universidad Nacional del Comahue, 2012

A THESIS SUBMITTED IN PARTIAL FULFILLMENT OF
THE REQUIREMENTS FOR THE DEGREE OF

MASTER OF APPLIED SCIENCE

in

The Faculty of Graduate and Postdoctoral Studies

(Electrical & Computer Engineering)

THE UNIVERSITY OF BRITISH COLUMBIA

(Vancouver)

August 2014

Abstract

Maximum Power Point Tracking (MPPT) strategies in Photovoltaic (PV) systems ensure efficient utilization of PV arrays. Among different strategies, the Perturb and Observe (P&O) algorithm has gained wide popularity due to its intuitive nature and simple implementation. However, such simplicity in P&O introduces two inherent issues, an artificial perturbation that creates losses in steady-state operation and a limited ability to track transients in changing environmental conditions. This work develops and discusses in detail an MPPT algorithm with zero oscillation and slope tracking to address those technical challenges. The strategy combines three techniques to improve steady-state behavior and transient operation: 1) idle operation on the Maximum Power Point (MPP), 2) identification of the irradiance change through a natural perturbation and 3) a simple multi-level adaptive tracking step. Two key elements, which form the foundation of the proposed solution, are investigated: the suppression of the artificial perturbation at the MPP and the indirect identification of irradiance change through a current-monitoring algorithm which acts as a natural perturbation. The Zero-oscillation, Adaptive step Perturb and Observe (ZA-P&O) MPPT strategy builds on these mechanisms to identify relevant information and produce efficiency gains. As a result, the combined techniques achieve superior overall performance while maintaining simplicity of implementation. Simulations and experimental results are provided to validate the proposed strategy and illustrate its behavior in steady state and transient operation.

Preface

This work is based on research performed at the Electrical and Computer Engineering department of the University of British Columbia by Francisco Paz, under the supervision of Dr. Martin Ordonez.

A first version of this work was presented in the 4th IEEE International Symposium on Power Electronics for Distributed Generation (PEDG), 2013 [1].

An extended version of this work was published in IEEE Transaction on Industrial Electronics [2].

As first author of the above-mentioned publications, the author of this thesis developed the theoretical concepts and wrote the manuscripts, receiving advice and technical support from Dr. Martin Ordonez, and developed simulation and experimental platforms, receiving contributions from Dr. Ordonez's research team.

Table of Contents

Abstract ii

Preface iii

Table of Contents iv

List of Figures vi

Acknowledgements viii

Dedication ix

1 Introduction 1

1.1 Motivation 1

1.2 Literature Review 2

1.2.1 Constant Relationship Algorithms 3

1.2.2 Hill Climbing Algorithms 4

1.2.3 Ripple Correlation Control 6

1.2.4 Model Based Algorithms 6

1.2.5 Heuristic-Based Algorithms and Other Special Algorithms 6

1.2.6 Summary 7

1.3 Contribution of the Work 7

1.4 Thesis Outline 9

2 System Background and Energy Harvesting Losses In PV Systems . . . 12

2.1 PV Panel Background . . . 13

2.2 Basic P&O Algorithm Background . . . 16

2.3 Steady-State Power Losses Estimation . . . 18

2.4 Irradiance Transient Power Losses Estimation . . . 21

2.5 Control System . . . 24

2.6 Summary . . . 25

3 Zero Oscillation Adaptive Perturb and Observe MPPT . . . 26

3.1 Idle Mode Operation . . . 27

3.2 Perturbation Direction and Magnitude Estimation . . . 28

3.3 Flowchart of the ZA-P&O MPPT . . . 29

3.4 Summary . . . 30

4 Simulations . . . 32

5 Experimental Results . . . 39

6 Conclusions . . . 46

6.1 Summary . . . 46

6.2 Future Work . . . 47

Bibliography . . . 48

List of Figures

1.1 Conceptual representation of the ZA-P&O MPPT 9

1.2 Issues with P&O technique 9

2.1 Block diagram of the PV system 12

2.2 PV cell model 14

2.3 VI/PV curves 15

2.4 Fill factor (FF) 16

2.5 Flowchart of the basic P&O MPPT algorithm. 17

2.6 Tracking losses on different operating conditions 18

2.7 Tracking efficiency for a transient 23

3.1 Idle mode operation illustrated 27

3.2 Irradiance change identification 30

3.3 Flow chart ZA-P&O 31

4.1 Trapezoidal irradiance profile 32

4.2 Simulations standard P&O with transient on raising edge 33

4.3 Simulations standard P&O with transient on falling edge 34

4.4 Simulations ZA-P&O with same transient 35

4.5 Efficiency of the PV panel for the ZA-P&O vs. standard P&O 37

4.6 Transient analysis in the phase V-I plane 38

5.1 Picture of the experimental set-up 39
5.2 Exp. capture of the standard P&O on rising edge 40
5.3 Exp. capture of the standard P&O on falling edge 41
5.4 Exp. capture of the ZA-P&O with the same transient 41
5.5 Steep/gradual trapezoidal irradiance profile 1 43
5.6 Steep/gradual trapezoidal irradiance profile 2 43
5.7 Exp. capture of the ZA-P&O with steep/gradual transient 1 44
5.8 Exp. capture of the ZA-P&O with steep/gradual transient 2 44

Acknowledgements

I would like to thank Dr. Martin Ordonez for his supervision. He established an outstanding example of leadership, mentoring, research, supervision and instruction.

I would like to thank my parents Cesar and Rosa, my sisters Carmen, Dolores and Carola and all of my family for their support, both moral and financial, during all my life and in particular during the past two years. Their constant presence in my life led me to this place.

I feel specially grateful for my girlfriend Celeste who supported me during this two years abroad with her constant encouragement. Her support in my decision to go for graduate studies, even when it would mean a long time apart, made this work possible. My special thanks and love go to her.

I would like to thank all the members of Dr. Ordonez's research group during the time of my Master's program (in order of position around the table): Matias Anun, Juan Galvez, Peter Ksiazek, Robert Cove, Jason Forbes, Ignacio Galiano, Navid Shafiei, Rafael Peña-Alzola and Ion Isbasescu. Their comments, discussion, suggestions, corrections, help and support made this work possible and always pushed me forward. If I don't take anything but the time shared with them, I would already be a better person.

I would also like to thank the University of British Columbia, the Faculty of Graduate and Postdoctoral Studies and the Electrical and Computer Engineering Department for the opportunity and support received during all this time. To all the faculty, administration and staff I feel grateful.

Finally, thank you for taking the time to read my thesis.

To all those I love.

Chapter 1

Introduction

1.1 Motivation

With the rising costs of oil and the concern surrounding global warming, the use of photovoltaic (PV) energy has been growing an average of 48% annually between the years 2000 and 2012 [3], with an cumulative a growth above 7,300%. PV array installations have been popularized in a variety of application and power levels, and can provide electricity either to isolated locations or contributing to the global grid through grid-tie inverters. Developments in power electronics topologies and control schemes that target PV applications present a special interest. In particular, a key element of the power conversion system is the Maximum Power Point Tracking (MPPT) algorithm. This control algorithm is responsible for finding the operating condition of the PV panel the yields the maximum possible power (known as Maximum Power Point, MPP). The MPP depends on the characteristics of the particular PV panel as well as the environmental conditions, such as the temperature (T) and the irradiance (G). On the one hand, the inherent characteristics of the PV panel change very slowly (mainly by aging or breaking) so they are not considered a concern in most MPPT algorithm; on the other hand, T and G change constantly just by the day/night cycle as well as by additional external events such as wind or shadows.

The most popular MPPT algorithms in industry are implemented by measuring the PV panel current and voltage and using that information to look for the MPP. The use of T and

G sensors is usually avoided due to the complexity and cost of such measurements. With this limited information, the changes in T and G present a challenge for the algorithms.

Once the MPPT algorithm has found the MPP, at the current T and G, the algorithm keeps the scanning perturbation in order to be able to identify a change in the PV characteristics. Most MPPT algorithms will make the PV panel work 50% the time outside the optimal condition causing some of the available energy not to be transferred to the load.

A transient in G occurs when the amount of light that arrives to the PV panel changes, therefore changing the characteristic curve and available power. Transients are produced by the natural day/night cycle (which produces slow transients) or by artificial object obstructing the path of the light (fast transients). During this periods, the MPPT algorithm needs to follow the MPP as the transient occurs and find it quickly once the transient has been extinguished. The industry-standard algorithms do not provide such feature without the need of adding a sensor to measure G.

Although the principal issues of the industry-standard MPPT algorithms are well documented in the literature, the impact of this effects is not treated with enough depth and a simple solution that mitigates this issues is not presented.

The work presented in this thesis provides a new improvement to MPPT techniques, which features a simple implementation and includes advanced characteristics such as the elimination of the steady state oscillation and the accurate tracking of transients.

1.2 Literature Review

Maximum Power Point Tracking (MPPT) for Photovoltaic (PV) applications is an active research in both academia and industry with more than 250 journal papers and 1600 conference papers available in IEEEXplore, and several commercial products in the market have included active MPPT algorithms. The existing literature discusses a variety of MPPT tech-

niques, circuits, applications and issues that help minimize the energy lost by not transferring it to the load but some issues remain unsolved.

As pointed out by the early works in the field [4–9], the MPPT process is based on finding the load impedance (as seen from the PV panel terminals) that matches the equivalent impedance of the PV panel. Before these early works, direct connection from the PV panel to the load was the common method, without the use of any impedance adaptation device. The economical advantage of using MPPT algorithms for PV applications was discussed in [10], showing that the energy transferred was highly incremented using power converters with this technology.

MPPT algorithms have a wide range of characteristics depending on the core application, ranging from very simple implementation to highly complex, from low to high precision. Simple algorithms are compact and can be implemented directly with analog circuits with very low consumption while high complexity algorithms are implemented using costly DSP for very large power applications. The principal contributions as well as the latest advances to the field are presented in the following paragraphs, highlighting the known issues that give a place to the present work.

1.2.1 Constant Relationship Algorithms

Some very simple algorithms, such as the Constant Voltage (CV), Fractional Open-Circuit Voltage (FOCV) [11–17] and Fractional Short-Circuit Current (FSCI) [4, 14–18] have the simplest implementation. The algorithm works by assuming a constant relationship between the open-circuit voltage (V_{oc}) or short-circuit current (I_{sc}) and the MPP voltage (V_{mpp}) or current (I_{mpp}). Such relationship is usually between 0.7 and 0.8 for a silicon solar cell. The algorithm then proceed to periodically measure the V_{oc} (or I_{sc}) and computing the corresponding optimal operating point. The precision of this algorithm is low compared with other advanced techniques and has the disadvantage of having to open the circuit

at the terminals of the PV panel in order to measure V_{oc} periodically (or short circuit it to measure the I_{sc}), which disturbs the operation of the load [14, 19]. Since the algorithms needs to constantly interrupt the operation of the PV panel these algorithms are not suitable to accurately track changing environmental conditions, since they would require a high frequency in the interruption conditions.

These techniques have been successfully implemented in extremely low power circuits like [20] and [21] boosting the energy harvested for autonomous equipment.

1.2.2 Hill Climbing Algorithms

The hill-climbing techniques are the most popular family of MPPT algorithms for industry applications due to the good balance between complexity, accuracy [22] and reliability [23]. These algorithms are based on scanning the Voltage-Current-Power characteristic curves in search for a determined condition that signals the MPP. One of these MPPT algorithms is the Incremental Conductance [22, 24–28], which periodically changes the operating point of the PV panel and compares the incremental conductance ($\Delta I/\Delta V$) to the DC conductance (I/V). These two variables have the same magnitude and opposite sign in the MPP, signaling the match of the impedance between load and source.

The other popular popular hill-climbing technique is the Perturb & Observe [27, 29–32]. This technique constantly changes the operating point and measures the change in the extracted power. It moves the operating point in the direction which causes the power to increment.

Both techniques offer a simple implementation but have some critical issues that make room for several improvements. The main disadvantages of this techniques have to do with the constant oscillation around the MPP [33, 34] even in steady state, the confusions that happen when the environmental conditions change [22, 28, 31, 35], the inability to adapt the tracking speed to different conditions and the presence of multiple local maxima. The basic

implementation of these algorithms are unable to stop oscillating in steady state (once the MPP has been found) since they need to keep scanning in case the environmental conditions change and a new MPP must be found. When the amount of light changes the amount of power yielded at a given operating point changes, the hill-climbing algorithms are unable to separate this change from the one produced by their own perturbation and often make wrong decisions leading to drifts from the MPP. For the basic algorithm the step-size of the perturbation is fixed, causing the scanning process to take very long when the MPP is far away from the current operating point. In large arrays, global maxima and local maxima can be different due to the effect of shadows cast over the panel. Since this algorithms use methods based on derivatives equal to zero, they are good only to find local maxima.

Some modified algorithms have been presented based on the hill-climbing algorithms, however these usually target one or more drawbacks while penalizing the others. Some examples of these modified strategies include the Adaptive Step variants of the P&O [29, 36–40] or InCond [41, 42], which apply some algorithm to change the step-size for fast tracking when away from the MPP and low oscillation when close to the maxima. This algorithm however, penalizes the detection of a change in the environmental conditions and can amplify this errors due to the step-size adaptation algorithm. The Plane Division (PD) method [43, 44] improves the speed of the standard InCon algorithm by creating a forbidden region, where the MPP cannot be located based on historical environmental data on the site and manufacturer information about the PV panel. Some modified versions of the hill-climbing algorithms [45–50] are able to find global maxima by modifying the algorithm, usually adding a second tracking stage. In [49], in addition to a second scanning stage, each cell's voltage is measure individually allowing for the identification of shaded cells. Recently, some strategies have been developed to overcome the confusion that results from changes in G [51, 52]. Opportunities to further improve steady-state behavior and provide an accurate tracking under changing G exist and are explored in this work.

1.2.3 Ripple Correlation Control

Since power converters have switching elements, their action introduces fluctuations in the extracted power causing the voltage and current to oscillate in each cycle. Some MPPT algorithms use this information in order to characterize the PV panel and find the MPP, this methods are known as Ripple Correlation Control (RCC) algorithms [53–58]. This algorithms provide accurate results without further oscillation, but the sensors implied need to be very precise since the oscillations from the point of view of the PV panel are small and fast, since the oscillation is present as speeds higher than the switching frequency. The cost of implementation of such algorithms is very high.

1.2.4 Model Based Algorithms

A different approach to MPPT algorithms is used by the Model-Based algorithms. These algorithms use a complex model of the PV panel and the measurement of voltage, current (and some times temperature and irradiance) to compute the optimal operating point. These usually leads to a very high precision (since an accurate model is being used) and tracking speed (since only a few steps are needed) but the complexity of the hardware and software become also very high (since it usually implies the resolution of implicit non-linear equations) [19, 59–62] or the use of heuristic methods to estimate the curve is needed [63]. These algorithms usually need a large amount of computational power per-step and a lot of information from the PV panel to be used.

1.2.5 Heuristic-Based Algorithms and Other Special Algorithms

Heuristic algorithm use principles derived from natural behavior to look for the MPP. Examples of these MPPT algorithms include the ones based in Artificial Neural Networks [29, 64–67], Fuzzy Logic [38, 66, 68–73], Particle Swarm Optimization [73–78],

Heurist-based algorithms are very popular when dealing with local maxima produced by partial shading [67, 79, 80]. Due to the training characteristics of these algorithms, a learning routine can be implemented that adapts in order to find the global maximum in a limited number of steps. However, these methods usually require resources and energy that might not be applicable to small-scale systems.

Finally, some applications allow for specific solutions that make use of the characteristics of the power converter [81, 82], such as the One Cycle Control in [83–85] for Grid connected systems. These strategies deeply connect with the nature of the controller to use as a evaluation criteria for the MPP. These algorithms are very specific of the topology under study.

1.2.6 Summary

As discussed in this literature review, there are a number of MPPT algorithms presented in the literature in the past 30 years. Many applications have benefited with the increment in processing power available and new techniques became available. However, most MPPT algorithms reported focus on constant environmental conditions and many challenges remain open. In particular an simple algorithm, comparable with hill-climbing, that is able to remove the oscillation in steady-state without compromising the tracking speed and accuracy and including a dynamical environmental conditions tracking is lacking in the literature. These technical challenges are addressed in this thesis and a zero oscillation adaptive track is investigated.

1.3 Contribution of the Work

The work presented in this thesis introduces a valuable MPPT strategy that contributes to mitigate the characteristic extraction losses present in PV electrical systems, as well as theo-

retical contributions to the quantization of the losses in steady state and transient conditions. The presented technique is simple and requires a small increment in the complexity of the code to implement it, making it a practical option for industrial applications. The following list summarizes the contributions of this work:

- The theory for a MPPT strategy referred to as Zero-oscillation, Adaptive-step Perturb and Observe (ZA-P&O), which reduces losses in steady-state and improves tracking under speed-varying changes in G is developed. The losses are reduced by suppressing the artificial perturbation around the MPP in steady-state, and are made possible by indirectly estimating a change in G through the natural perturbation introduced by the error on a Proportional-Integral (PI) controller and the change in current in the operating point. Estimating the change enables the perturbation step to be adjusted in order to accurately track the changes in the MPP. The main advantages of this combined strategy are conceptually presented in Fig. 1.1 and compared with the standard P&O in Fig. 1.2. The improvements of the proposed strategy are summarized as follows: ❶ the efficiency in steady state is improved by suppressing the oscillation, ❷ the confusion caused by a change in G is eliminated and ❸ the step is adjusted for accurate tracking.

- A study of the nature of the extraction losses both in steady state and transient is performed and an estimation of those values is performed. The losses are quantized in steady state as a function of the PV cell parameters and the step size of the MPPT algorithm. The losses during the transient are quantized, for a fixed step size, as a function of the slope of the change in G, between two fixed levels. This figures allow the visualization of the need for the ZA-P&O MPPT strategy.

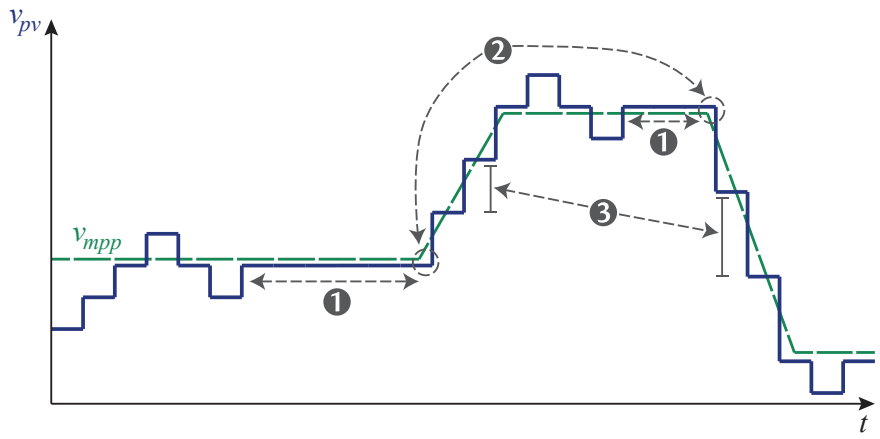

Figure 1.1: Conceptual representation of the ZA-P&O combined MPPT strategies: efficiency maximized with no oscillation ❶, correct decision ❷ and step adjustment ❸ under changes in irradiance.

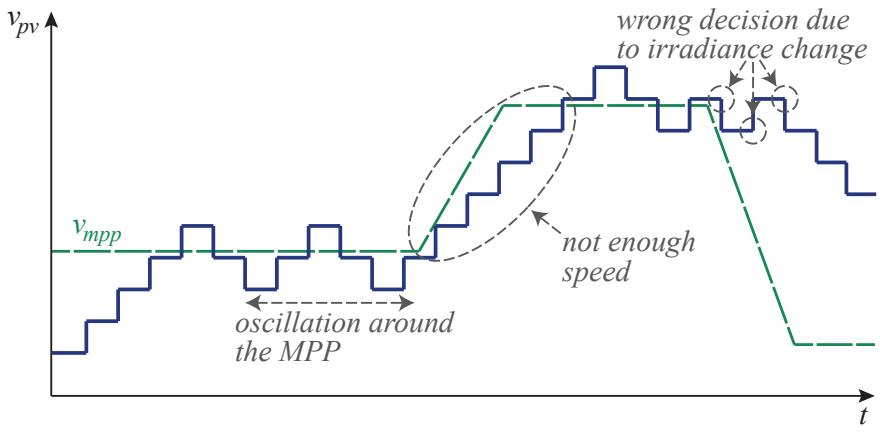

Figure 1.2: Issues with P&O technique: oscillation in steady state, wrong tracking step and confusion during irradiance change.

1.4 Thesis Outline

The present work is organized in the following way:

- In Chapter 2, the characteristics of a PV powered system are presented as well as the different conditions that cause some of the energy harvested by the PV panel not to be transferred to the load. The basic concepts of a PV panel are introduced in Section 2.1. The basic P&O algorithm is explained in Section 2.2 as a reference tool to compare the proposed algorithm. The losses in steady state, which are inherent to the MPPT strategy, are studied in Section 2.3. The amount of energy lost is quantized as a function of the step size selected for the tracking process. In Section 2.4, the power losses during transient conditions in the irradiance are studied and the effect of the mismatch between the speed at which the MPP moves and the speed at which the strategy tracks it is quantized. The basic concepts of the implemented control system and its impact on the proposed MPPT algorithm are explained in Section 2.5.

- In Chapter 3, the ZA-P&O MPPT strategy is introduced. The proposed strategy reduces the losses in steady state by eliminating the constant oscillation, characteristic of the regular MPPT algorithms producing a clean behavior once the MPP was reached . The losses that are produced during transients in the irradiance are reduced by indirectly estimating this change and adjusting the tracking step to match the direction and slope of the transient. The resulting transient closely tracks the MPP during irradiance changes.

- The simulation validation of the ZA-P&O is presented in Chapter 4 using simulations and an experimental set-up. The simulations compare the ZA-P&O with the standard P&O algorithm in order to point out the advantages of the proposed strategy. These results show the elimination of the losses in steady state and the reduction of the losses during the transient.

- Further validation of the proposed strategy is presented with several captures of the experimental results in Chapter 5. The different features are tested using the same

profile for G and both algorithms and compared with the simulation results. Addition profiles are presented and tested using the ZA-P&O algorithm to illustrate the step adaptation features.

- Lastly, in Chapter 6 a summary and conclusion of this work is presented, along with some details of the future research opportunities.

Chapter 2

System Background and Energy Harvesting Losses In PV Systems

A typical PV power conversion system includes a PV array connected to a power converter that charges a battery or is connected to the grid. The objective of the converter is both to change the characteristics of the PV voltage/current to the needs of the load and to adapt the impedance seen from the PV panel to ensure maximum power extraction. The block diagram of the implemented system is presented in Fig. 2.1. It includes a PV panel supplying energy through a power converter to a load, formed by a battery bank. The batteries are assumed

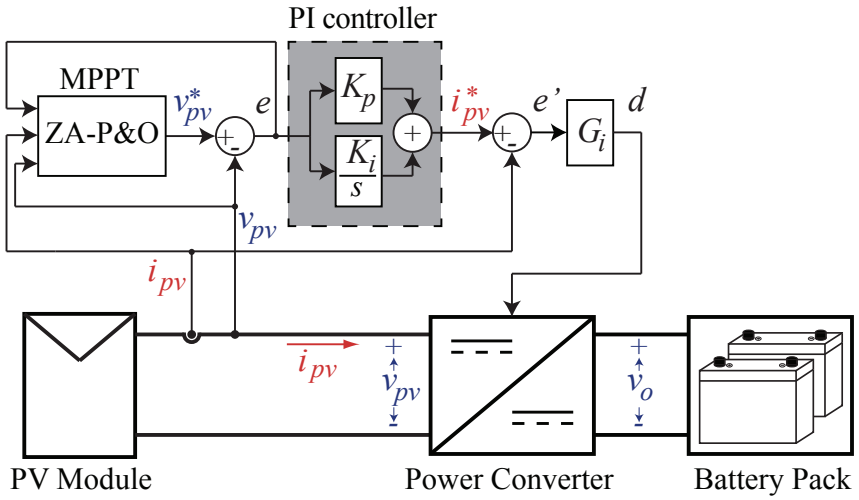

Figure 2.1: Block diagram of the PV system, the PV panel is connected to a battery bank through a DC/DC power converter, the control system regulates the PV voltage to match the instructions of the MPPT block.

to be discharged, and therefore able to absorb all the available power without influencing the MPPT process. The PV panel voltage and current (v_{pv},i_{pv}) are regulated by the controller to achieve the maximum power extraction determined by the ZA-P&O MPPT strategy. The DC/DC converter has a boost topology that ensures continuous current from the PV panel, minimizing the losses due to the current ripple.

In this chapter the model of the PV panel is presented. A summary of the basic P&O and its limitations is discussed. The losses due to the inaccuracy of MPPT are derived, showing the need to develop an improved MPPT strategy that minimizes the losses in steady state and boosts the accuracy of the tracking under changing environmental conditions. Finally, the concepts behind the implemented control loops are presented, introducing the natural perturbation concept that allows the elimination of the steady state oscillations and and enables the dynamic adjustment of the step size in proportion to the change in G. The proposed ZA-P&O strategy builds on this foundation.

2.1 PV Panel Background

The equivalent circuit for a PV cell is presented in Fig. 2.2 [86], including the effects of the series resistor (R_s) and the shunt resistor (R_{sh}). The diode D is characteristic of the P-N junction of the cell structure, while the photocurrent (i_G) is produced by the light photons arriving at the junction. The basic PV panel equations are reviewed to provide a clear background for the estimation of losses due to the MPPT strategy operation. For a PV panel built with M parallel strings of N cells connected in series, the panel's current (i_{pv}) at any given voltage (v_{pv}), temperature (T) and irradiance (G), neglecting the resistors, is given by [61]

$$i_{pv} = Mi_G - MI_0 \left(\exp\left(\frac{v_{pv}}{NnkT/q} \right) - 1 \right). \tag{2.1}$$

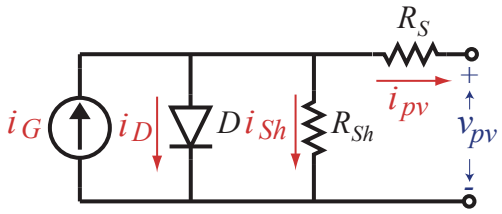

Figure 2.2: Photovoltaic (PV) cell model including the parasitic effects of the series resistor (R_s) and the shunt resistor (R_{sh}), the photocurrent (i_G) is proportional to the irradiance (G).

where I_0 is the reverse saturation current of D, q is the electron charge, n is the diode factor, k is Boltzmann's constant (in joules per kelvin), T is the PV panel temperature (in kelvin) and i_G is proportional to G

$$i_G = \gamma G. \tag{2.2}$$

This relationship determines the influence of the environment variables (G,T) in the nonlinear cell characteristics and is fundamental to develop a MPPT strategy that can track this changes. Two other basic magnitudes are of special interest when describing a PV cell and will be used to quantify the MPPT strategy behavior: the open-circuit voltage (V_{oc}) and the short-circuit current (I_{sc}). The V_{oc} is defined as v_{pv} when i_{sc} is null:

$$\begin{aligned} V_{oc} &= v_{pv}|_{i_{pv}=0} \\ &= \frac{NnkT}{q} \ln\left(\frac{i_G}{I_0} + 1\right). \end{aligned} \tag{2.3}$$

On the other hand, I_{sc} is defined as the i_{pv} when v_{pv} is null:

$$\begin{aligned} I_{sc} &= i_{pv}|_{v_{pv}=0} \\ &= M i_G. \end{aligned} \tag{2.4}$$

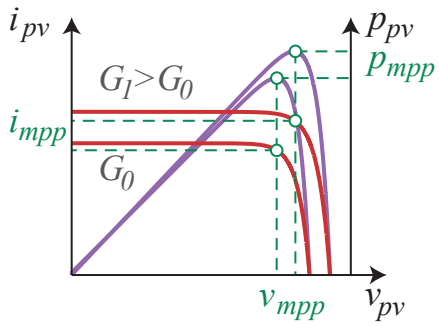

Figure 2.3: Characteristic I-V and P-V curves of the a PV cell under different irradiance conditions.

The characteristic I-V and P-V curves for a PV cell are shown in Fig. 2.3, the operating condition (v_{mpp},i_{mpp}) that yields the maximum available power (p_{mpp}) is called the Maximum Power Point (MPP). When the environmental conditions (G, T) change, the characteristic curves of the PV panel change and the MPP moves. The MPPT algorithm must not only be able to find the MPP in stationary environmental conditions, but to track it while it changes.

A final magnitude to characterize the PV panel is useful, the fill-factor (FF). The FF is defined as the ratio between the MPP power and the product of V_{oc} and I_{sc}

$$FF = \frac{I_{mpp}V_{mpp}}{I_{sc}V_{oc}}, \tag{2.5}$$

indicating how much the actual PV panel differs from an ideal Voltage/Current source. The FF is illustrated in Fig. 2.4, a good PV panel will have a Fill factor between 0.75 and 0.90. Aging and damages can reduce this value.

Both the change in G and in T influence the characteristics of the PV panel, but they do so in different ways. From the basic expressions (2.1)-(2.4) each influence can be quantified and studied. A change in G mostly affects I_{sc}, which increases proportionally to G, while V_{oc} remains almost the same as in Fig. 2.3 (for example, doubling G increases I_{sc} by 100% while V_{oc} only increases by 3%). On the other hand, changes in T mostly affect V_{oc} while

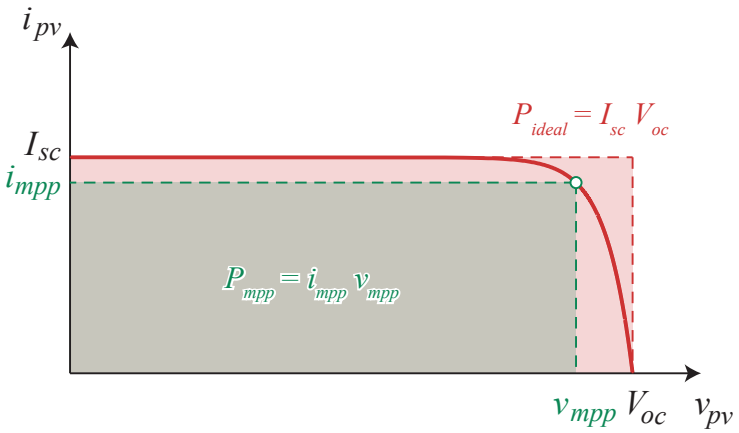

Figure 2.4: The Fill Factor (FF) of the PV panel is defined as the ratio between the maximum power (p_{mpp}) and the ideal power that could be extracted from the cell ($V_{oc}I_{sc}$).

I_{sc} is less affected (for example 1 K variation increases I_{sc} by 0.06% and V_{oc} is decreased by 0.4%). However, large gradients are expected from G due to clouding and shades, while T is expected to have a smaller gradient. The present work will focus only on the change in G with different dynamics (fast and slow) during the transient.

2.2 Basic P&O Algorithm Background

The flowchart of the basic P&O MPPT algorithm is presented in Fig. 2.5. The basic P&O scans the P-V curve of the panel in search for the MPP by changing the operating point (v^*_{pv} or i^*_{pv}), which is known as perturbation step, and then measuring the change in P (ΔP), known as observation step. If ΔP is greater than zero, then a new perturbation is introduced in the same direction. If ΔP is lower than zero, the direction of the perturbation is changed. The P&O keeps searching for the MPP until it has found an operating point such that ΔP is lower than zero in any direction; this condition is called steady-state. The P&O keeps perturbing the system in order to detect a change in the MPP (caused by a change in the environmental conditions), which triggers a new scan. An illustration of this process can be observed in Fig. 1.2. This steady-state perturbation drifts the operating point away from the

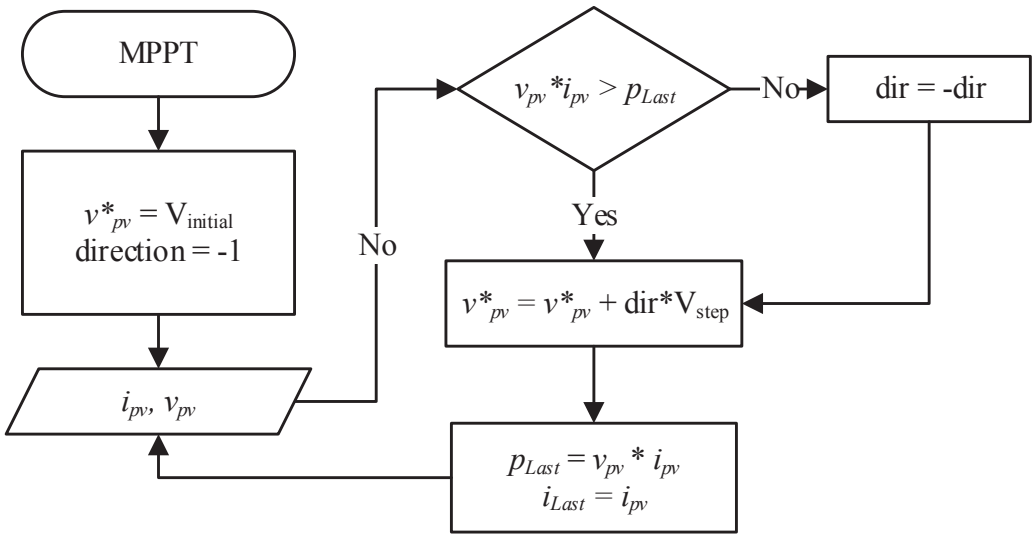

Figure 2.5: Flowchart of the basic P&O MPPT algorithm.

MPP; this introduces losses. In theory, this perturbation can be reduced, reduced in order to keep the detection feature but minimize power losses. However, such a small perturbation would require extremely precise sensors to measure the change in power. Therefore, the perturbation in steady state (if kept) has a minimum amplitude that depends on the sensors.

Every time there is a change in the environmental conditions, there is a change in the P at the established operating point that masks the change caused by the perturbation. In this condition, the P&O algorithm might be induced to respond as though the perturbation introduced produced an effect different than the true one. As observed in Fig. 1.2, during the transient on the right (MPP moves to a lower voltage), since G is reduced, the overall P is reduced, regardless of the direction of the perturbation. In this condition, the P&O algorithm changes direction in each step, trapping the system until the transient finishes.

Finally, the classic P&O algorithm has a fixed step size, and therefore can only accurately track the change in the MPP when it moves at a given rate (providing it made the decision for the correct direction). The quantification of these losses is estimated in this thesis.

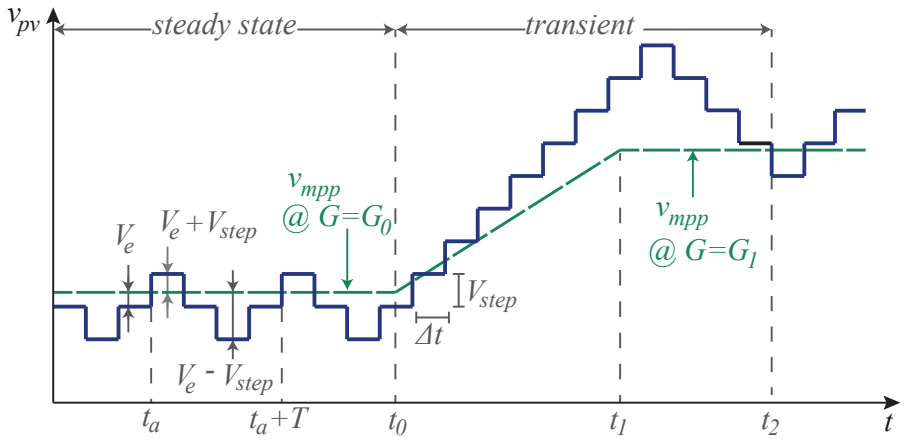

Figure 2.6: The tracking losses depend on the different operating conditions (steady state or irradiance change).

The above mentioned issues present serious drawbacks to the P&O algorithm; the ZA-P&O MPPT tackles those limitations, as will be explained in Chapter 3.

2.3 Steady-State Power Losses Estimation

The proposed MPPT strategy removes the oscillation around the MPP in steady state that is introduced by the artificial perturbation, and adapts the steps during a transient to accurately track the MPP in order to reduce the available power lost. A typical operation situation of a PV panel is displayed in Fig. 2.6, including a period in which G remains constant and a transient. The power losses in different stages of the MPPT (steady state or transient) are given by different expressions.

The power losses (P_r) in relationship with the available power (P_{mpp}) in steady state for the MPPT algorithms can be estimated as [33]

$$\frac{P_r}{P_{mpp}} \approx \left(\frac{(\Delta v_{pv})_{RMS}}{v_{mpp}}\right)^2 \left(1 + \frac{v_{cell}}{2nkT/q}\right), \tag{2.6}$$

where $(\Delta v_{pv})_{RMS}$ is the RMS value of the voltage oscillation and v_{cell} is the MPP voltage of each cell in the panel (around 0.5 V). As shown in the following equations, derived as part of this thesis, (2.6) can be manipulated to compare the losses in steady state for the traditional P&O with the ZA-P&O. A cycle of the voltage oscillation around the MPP for the P&O is given by

$$\Delta v_{pv}(t) = \begin{cases} V_e + V_{step} & \text{if } 0 < t \leq T/4 \\ V_e & \text{if } T/4 < t \leq T/2 \\ V_e - V_{step} & \text{if } T/2 < t \leq 3T/4 \\ V_e & \text{if } 3T/4 < t \leq T, \end{cases} \tag{2.7}$$

where V_e is the difference between V_{mpp} and the closest v_{pv} set by the MPP tracker, due to the step size (see Fig. 2.6, in steady state). As can be observed, V_e is related to V_{step} by

$$V_e = bV_{step}, \tag{2.8}$$

where b is a number between -0.5 and 0.5. Therefore (2.7) can be expressed as

$$\Delta v_{pv}(t) = \begin{cases} (b+1)V_{step} & \text{if } 0 < t \leq T/4 \\ bV_{step} & \text{if } T/4 < t \leq T/2 \\ (b-1)V_{step} & \text{if } T/2 < t \leq 3T/4 \\ bV_{step} & \text{if } 3T/4 < t \leq T. \end{cases} \tag{2.9}$$

The RMS value of the voltage oscillation for the P&O is

$$\begin{aligned}(\Delta v_{pv})_{RMS}^{P\&O} &= \sqrt{\frac{1}{T}\int_0^T \Delta v(t)^2 dt} \\ &= V_{step}\sqrt{\frac{1}{4}((b+1)^2 + 2b^2 + (b-1)^2)} \\ &= V_{step}\sqrt{\frac{1}{2} + b^2}. \end{aligned} \tag{2.10}$$

If the voltage is kept as close as possible to the MPP (no oscillation), the RMS value of the voltage is

$$(\Delta v_{pv})_{RMS}^{0} = bV_{step}. \tag{2.11}$$

Replacing (2.10) in (2.6) gives the relative losses for the P&O algorithm in steady state

$$\left(\frac{P_r}{P_{mpp}}\right)_{P\&O} \approx \left(\frac{1}{2} + b^2\right)\left(\frac{V_{step}}{v_{mpp}}\right)^2 \left(1 + \frac{v_{cell}}{2nkT/q}\right). \tag{2.12}$$

Plugging (2.11) in (2.6) gives the relative losses when the algorithm does not oscillate.

$$\left(\frac{P_r}{P_{mpp}}\right)_0 \approx b^2 \left(\frac{V_{step}}{v_{mpp}}\right)^2 \left(1 + \frac{v_{cell}}{2nkT/q}\right). \tag{2.13}$$

The ratio between (2.12) and (2.13) indicates the extra power lost by keeping the oscillation in steady state

$$\frac{(P_r/P_{mpp})_{P\&O}}{(P_r/P_{mpp})_0} \approx \frac{1/2 + b^2}{b^2} = 1 + \frac{1}{2b^2}. \tag{2.14}$$

As just demonstrated, (2.14) indicates that the losses in steady state are incremented by $1/2b^2$ because of the oscillation. In the best case, with $b = 0.5$, the losses are three times larger if the oscillation is maintained.

For a PV panel with $V_{oc} = 200$ V and $I_{sc} = 1$ A, v_{mpp} is around 170 V, the cell voltage at the MPP is around 0.5 V and with $V_{step} = 2$ V (1% of V_{oc}). The relative losses (expressed

in percentage) using the $P\&O$ are obtained evaluating (2.12) for these specific values

$$\left(\frac{P_r}{P_{mpp}}\right)_{P\&O} \approx 0.09\%. \tag{2.15}$$

That means the oscillation around the MPP causes a 0.09% power losses. For the same PV panel, if the oscillation is removed in steady state, the losses and can be estimated as

$$\left(\frac{P_r}{P_{mpp}}\right)_0 \approx 0.03\%. \tag{2.16}$$

This configuration losses only 0.03% of the available power, three times less than does the traditional P&O. Projected in a 25 years life cycle of the PV setup this means a tangible benefit in overall energy production.

2.4 Irradiance Transient Power Losses Estimation

The following equations are derived in this thesis to quantify the losses due to dynamic MPPT error. During a transient in G, the MPP will move. The standard P&O algorithm has a fixed V_{step} and sampling time Δt; therefore it is able to accurately track only one slope of G, as seen in Fig. 2.6. If G changes more rapidly, the tracking would be inaccurate during the transient and would have to reach the MPP after the ramp stops. If G changes more slowly, the operating point would drift away from the MPP until the ramp stops, after which it would have to reach the true MPP (see Fig. 2.6).

During a ramp change in G from G_0 at t_0 to G_1 at t_1, G can be expressed as

$$G(t) = \begin{cases} G_0 & \text{if } t \leq t_0 \\ G_0 + (t - t_0)\delta G & \text{if } t_0 < t \leq t_1 \\ G_1 & \text{if } t_1 < t. \end{cases} \tag{2.17}$$

Then, the power extracted from the PV panel during the transient is given by

$$p_{pv}(t) = v_{pv}(t) \left(\gamma G(t) - I_0 \left(\exp\left(\frac{v_{pv}(t)}{nkT/q} \right) - 1 \right) \right). \tag{2.18}$$

A comparison with the maximum power (obtained while operating constantly at v_{mpp})

$$p_{mpp}(t) = v_{mpp}(t) \left(\gamma G(t) - I_0 \left(\exp\left(\frac{v_{mpp}(t)}{nkT/q} \right) - 1 \right) \right), \tag{2.19}$$

shows the loss due to inaccurate tracking. The instantaneous tracking efficiency is given by

$$\eta_{MPPT}(t) = \frac{p_{pv}(t)}{p_{mpp}(t)}, \tag{2.20}$$

however, sometimes it is more important to have a more general overview of the losses. Computing the energy obtained through the transient (E_{pv}) and comparing it with the energy that would be obtained if the panel had always operated at the MPP (E_{mpp}) , enables the average tracking efficiency ($\bar{\eta}_{MPPT}$) to be quantified

$$\bar{\eta}_{MPPT} = \frac{E_{pv}}{E_{mpp}} = \frac{\int_{t_0}^{t_2} p_{pv}(t)dt}{\int_{t_0}^{t_2} p_{mpp}(t)dt}. \tag{2.21}$$

Numerically integrating these expression for a given PV panel using a P&O with a fixed Δt and V_{step} shows how $\bar{\eta}_{MPPT}$ is minimal for a certain δG.

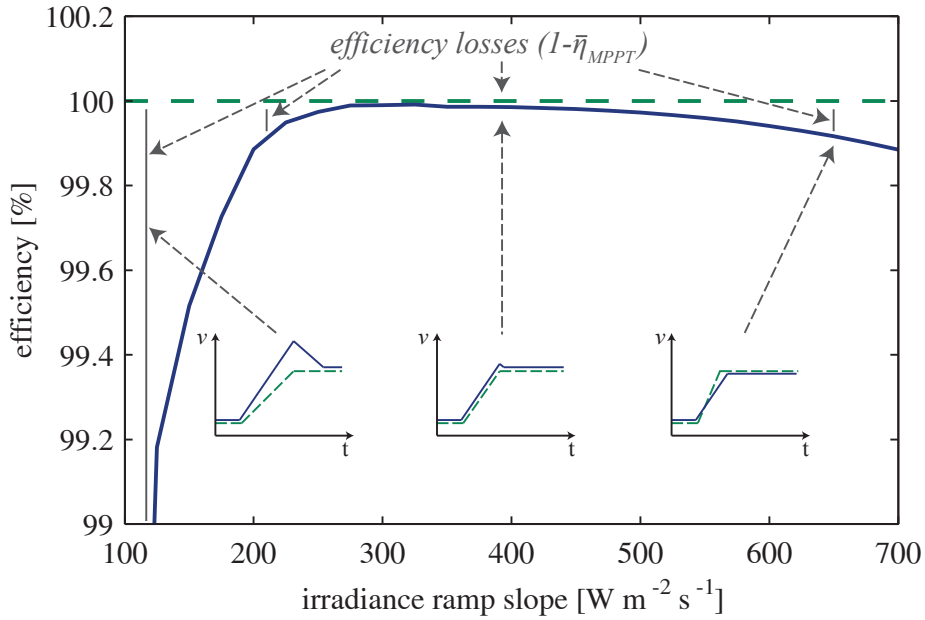

Figure 2.7: Tracking efficiency ($\bar{\eta}_{MPPT}$) for a transient between $G_0 = 600$ Wm^{-2} to $G_1 = 1000$ Wm^{-2}, for a P&O algorithm with $\Delta t = 1$ s and $V_{step} = 2$ V showing the losses when the MPPT slope does not match the slope produced by δG.

These equations derived in this thesis provide valuable insight into the transient losses. The results for the example PV panel when G is changing from $G_0 = 600$ Wm^{-2} to $G_1 = 1000$ Wm^{-2} with several different δG are displayed in Fig. 2.7. The small sketches in Fig. 2.7 illustrate the tracking process with different slopes of G and a fixed step size: when the slope is slower than the steps, the tracking point overshoots; when the slope is higher than the steps, the tracking point takes time to catch up. There is one slope where the tracking point closely follows MPP. The power losses are minimal for a slope of 300 Wm^{-2}s^{-1}; this is the slope that the P&O can accurately track. If the slope is lower than the optimal, for example $\delta G = 100$ Wm^{-2}s^{-1}, v_{pv} will become larger than v_{mpp} leading to larger losses in the order of 3% (since the PV curves steeper for higher voltages as seen in Fig. 2.3). When the slope is higher and the MPPT lags behind, for example for $\delta G = 600$ Wm^{-2}s^{-1}, the losses are around 0.1%. It is clear that a MPPT strategy that has a fixed step for tracking is not

optimal during transients, and an adaptive strategy will ensure a closer tracking of the MPP in this condition, independent of the change in G.

2.5 Control System

Unlike most power converters, where the controller aims to regulate the output voltage, for MPPT purposes the controller regulates the input of the converter (v_{pv}). The controller is shown in Fig. 2.1. It uses a dual loop to regulate both i_{pv} and v_{pv}, this is then used to obtain additional information regarding the change in environmental conditions, a natural perturbation to the system. The inner loop (faster) will regulate i_{pv} by setting the duty cycle (d) of the converters switches. The outer loop, slower regulates v_{pv} to the level determined by the MPPT strategy (v_{pv}^*) by setting the reference current (i_{pv}^*).

The use of a dual-loop controller serves two purposes. On the one hand, it improves the stability of the system. On the other hand, it helps isolate the change in G acting as a natural perturbation to lead the MPPT. This avoids the use of a continuous artificial perturbation in steady state to track this change.

Since v_{pv}^* is updated at the sampling speed of the MPPT (slower than the control system), during a sudden change in G, the outer loop will keep v_{pv} constant by changing i_{pv}. This change in i_{pv} indicates the change in G and acts as a natural perturbation. Moreover, it is shown in [52] that when G changes with a slope δG during the sample period (Δt) and the voltage loop has a PI controller the tracking error (e) is proportional to δG

$$e \propto \frac{\delta G}{K_i}. \tag{2.22}$$

Using this information, the proposed MPPT strategy can stop the artificial perturbation in steady state and monitor the change in i_{pv} and e (natural perturbation) to determine the change in the environment and adjust the step size (V_{step}).

2.6 Summary

In this chapter, the block diagram of the system was studied. The characteristics of the PV panel and a industry-standard MPPT algorithm were presented in order to introduce further details. The characteristic losses produced by MPPT algorithms in steady state and transient conditions were presented and a means to evaluate them was introduced. Finally, the control technique and its impact on the proposed MPPT strategy was presented. The effects of a transient in G are seen as a natural perturbation, that allows the removal of the artificial perturbation characteristic of the P&O. In the following chapter, an advanced MPPT strategy will be introduced that uses this characteristics to eliminate the oscillation in steady-state (reducing the losses) and uses the controller signals to infer the direction and magnitude of the change in G and produce an accurate tracking of transients.

Chapter 3

Zero Oscillation Adaptive Perturb and Observe MPPT

The traditional hill-climbing algorithm (P&O) discussed in the previous chapter has a number of disadvantages such as an oscillation in steady state (due to the continuous scanning process), it gets confused during changes in G and is unable to identify the rate of change of the irradiance and adapt the step-size correctly, this introduces losses to the system that were also identified in the previous chapter. The ZA-P&O MPPT strategy is developed based on two key aspects: 1) detection of the steady-state operation and 2) determination of the direction and magnitude of the perturbation. In steady-state, the standard P&O algorithm will oscillate around the closest possible voltage (due to quantization of the voltage step) in three levels, as in Fig. 1.2. This introduction of an artificial perturbation allows the MPPT to scan the curve for a change in the characteristics caused by environmental conditions. The ZA-P&O identifies this situation and establishes the operating point (v_{pv}^{*}) in the closest value, as shown in Fig. 1.1. In this operating mode, called idle mode, the losses are minimized as shown in Section 3.1. The environmental change is identified by monitoring the error in the PI controller (e) and the change in current (i_{pv}), which generate a natural perturbation clearly correlated to the change in the conditions. The use of this natural perturbation enables a cleaner operation, removing redundant oscillations that are convoluted with the information of environmental change and can cause confusion. This allows tracking

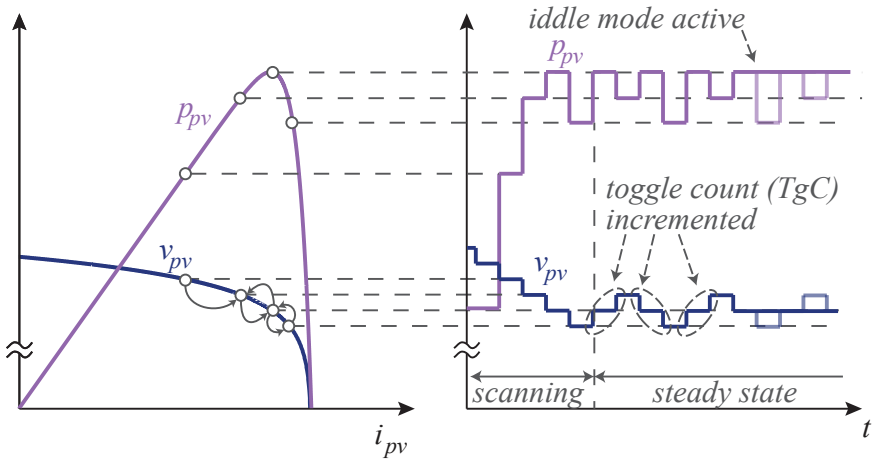

Figure 3.1: Illustration of the Idle mode operation. On the left, the V-I plane shows the characteristic curve and the tracking process; on the right, the time domain correspondence is shown. The idle mode detects the oscillations and activates the idle mode eliminating the losses.

to reactivate when necessary and to establish an accurate step size based on the known slope, instead of toggling continuously as is usually done.

3.1 Idle Mode Operation

Conventional MPPT strategies search for the MPP by periodically changing v_{pv} and measuring the effect over p_{pv} or some other parameter. Since no way of identifying a change in G (and the corresponding displacement of the MPP) is included in the MPPT strategies, it must keep perturbing the operating point even when the MPP has been found (steady-state). This is reflected in a three-level operating condition shown in Fig. 1.2, where the operating point toggles around the closest voltage allowed by the discrete steps. This is an artificial perturbation that reduces the efficiency of the energy extraction.

The ZA-P&O MPPT strategy uses a natural perturbation, native to the control of the system: the change in i_{pv} and the error in the PI controller (with constant v_{pv}^{*}), making it possible to eliminate the artificial perturbation. The proposed method identifies the oper-

ation in steady state by counting consecutive changes in direction with a common middle point (v_{mid}). When a step is introduced in v^*_{pv}, if the step is the second in the same direction and the power increased, the algorithm displaces v_{mid}. The software computes one toggle and registers it in the toggle counter (TgC) each time the set point returns to v_{mid}. The maximum number of toggles around v_{mid} before activating the idled mode and removing the perturbation is set as a parameter (TgM) and is used to avoid confusion caused by noise.

The operation of the idle mode is illustrated in Fig. 3.1. On the left side, the V-I plane curves are shown; the corresponding time domain progression is displayed on the right. During the tracking phase, when the operating voltage is away from the MPP, the steps are always in the same direction and therefore the toggle counter is not incremented. When v_{pv} reaches the MPP it starts oscillating around a middle point. The MPPT algorithm detects this condition and increments the counter. Once the maximum number of counts allowed is reached, the Idle mode is activated and the tracking process stops. In a lighter shade, it can be observed how the MPPT would continue oscillating if the Idle mode was not implemented leading to losses in the system.

3.2 Perturbation Direction and Magnitude Estimation

As explained in Section 2.5, the implemented controller can be used to monitor the changes in the environmental conditions. This leads to accurate knowledge of the magnitude of the change in G and the slope δG. This can be directly correlated to the displacement of v_{mpp} and i_{mpp}. This information provides the correct direction to the ZA-P&O.

In case of a slope change in G it is not enough to know the direction of the displacement. If the slope is too small, the MPPT may detect the change and introduce a step that will lead the operating point far away from the MPP. If the slope is too steep, the steps may not be large enough to track the MPP. Since the magnitude of the slope can be identified

from (2.22), the magnitude of the change in i_{pv} that results from the change in G is known as

$$\Delta i_{pv} = K_i e \Delta t \tag{3.1}$$

where Δt is the sample time of the MPPT strategy. As can be seen, from the measurement of e and the knowledge of K_i and Δt, it is possible to know the change in i_{pv}, proportional to the change in G. In this condition, we can adjust the step in proportion to the change in the G. The value of the proportionality constant depends on the PV panel.

The identification of the change in G is illustrated in Fig. 3.2. In the upper part of the the illustration, target voltage v_{pv}^* and the actual PV panel voltage v_{pv} are presented. The PV panel is commanded to change the operating point in the characteristic three-level operation. In the bottom of the graph, a profile in G is shown: in the first part G keeps constant and then it starts increasing with a certain slope δG; finally it starts decreasing with a different slope. Observing v_{pv}^* and v_{pv} it can be seen that there is a tracking error during the slope changes in G and the amplitude of this error is proportional to the slope. Since the error signal is automatically available from the implementation of the controller, this signal can be fed to the MPPT and used to determine the correct direction.

3.3 Flowchart of the ZA-P&O MPPT

The flow chart for the ZA-P&O is presented in Fig. 3.3. The strategy includes tunable parameters, such as the thresholds for the current change and error (i_{Th} and e_{Th}) and the number of toggles around the MPP required to establish the idle mode (TgM). This thresholds are included in order to prevent the algorithm to get confused by the noise in the sensors. Outside the special conditions established of Idle mode and identification of the change in G, the

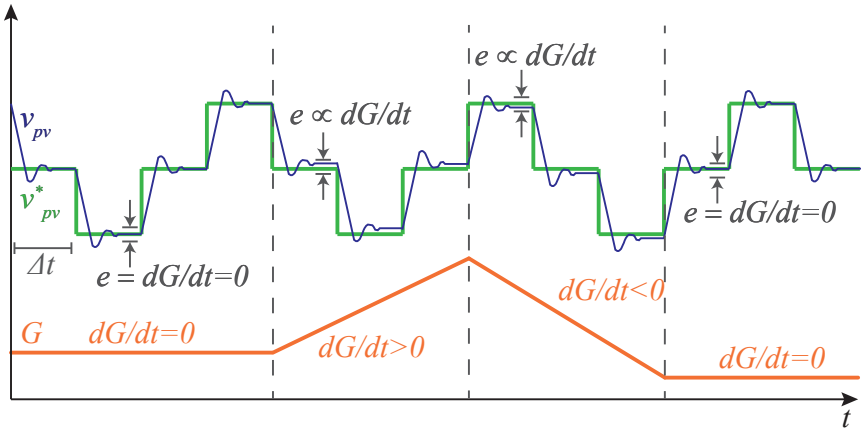

Figure 3.2: The change in irradiance is identified via the tracking error in steady state caused by the slope of the irradiance change.

algorithm works as a P&O. As can be observed, the blocks added to the algorithm are based on comparisons and simple operations and do not add major complexity to the algorithm which leads to a simple implementation comparable with the standard P&O.

3.4 Summary

In this chapter, an advanced MPPT strategy was proposed. The ZA-P&O MPPT strategy combines two key elements discussed previously to enhance the standard P&O algorithm with new features. The Idle mode was introduced, that allows the MPPT to stop once it has reached the MPP instead of constantly oscillating, reducing the losses in steady-state. This is possible due to the implementation of an indirect estimation of the change in environmental conditions via the control law of the converter. An additional benefit of this estimation is the ability to identify the occurrence of a change in G, its direction and the magnitude of the slope allowing for accurate tracking of the MPP during the transients. Validation of the ZA-P&O MPPT is provided in the next two chapters, first with simulations and then with experimental captures.

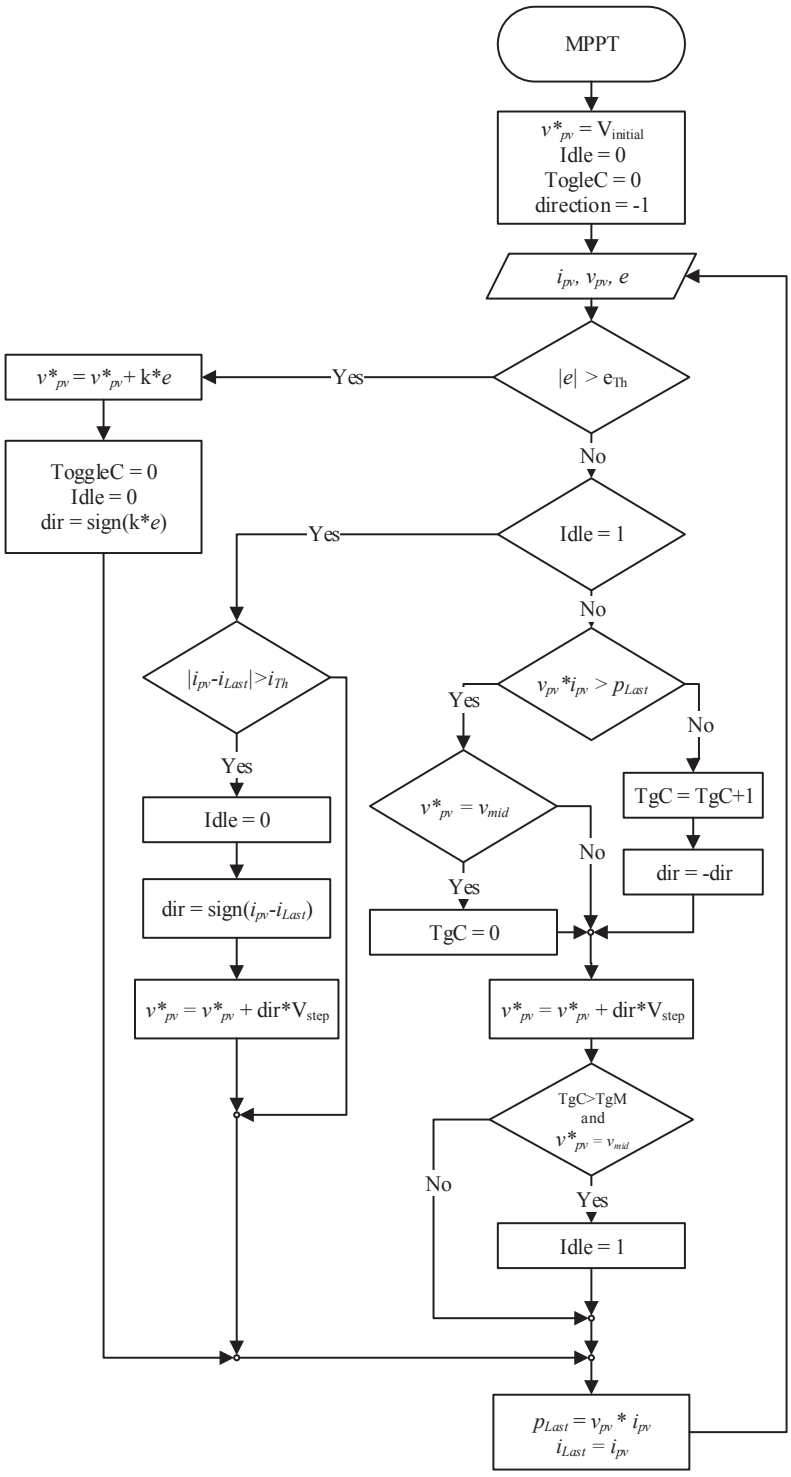

Figure 3.3: Flow chart for the ZA-P&O MPPT strategy.

Chapter 4

Simulations

In the previous chapter, the ZA-P&O MPPT was introduced. This algorithm adds new features to the standard P&O algorithm and creates an important improvement in terms of steady-state oscillation and transient tracking. To validate these improvements, a computer model and a profile of G were generated to test the known issues of the regular P&O against the ZA-P&O MPPT algorithm.

The results of the computer simulation for both the ZA-P&O MPPT and the standard P&O for a trapezoidal irradiance (G) profile are presented in this chapter. The model consists of a PV panel that can be configured to perform with the desired characteristics,

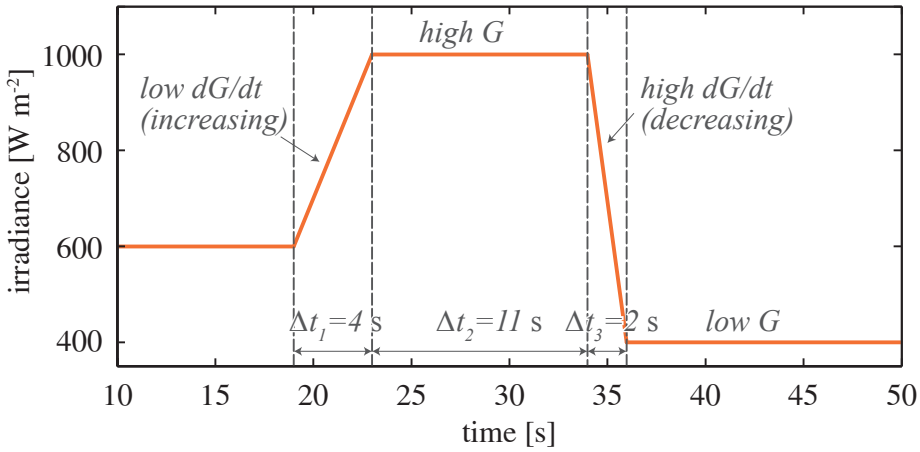

Figure 4.1: Trapezoidal irradiance (G) profile used to simulate the P&O algorithm and the proposed ZA-P&O strategy.

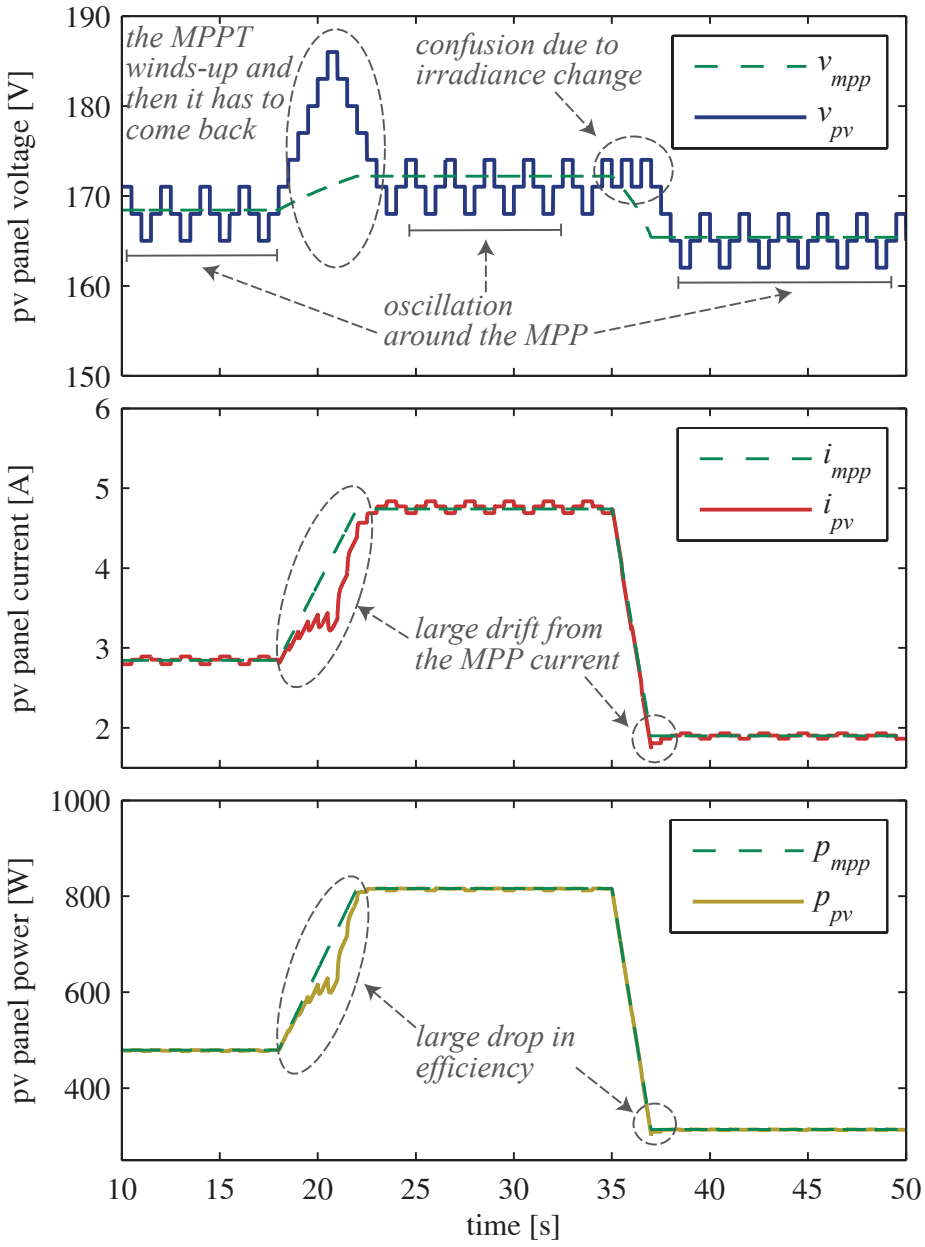

Figure 4.2: Standard P&O issues when the irradiation (G) slope starts during a raising step of the algorithm for v_{pv}, i_{pv} and p_{pv}.

a PI controller to regulate the voltage of the PV panel, and the MPPT to determine the operating point. The output of the PI controller sets the current in the PV panel.

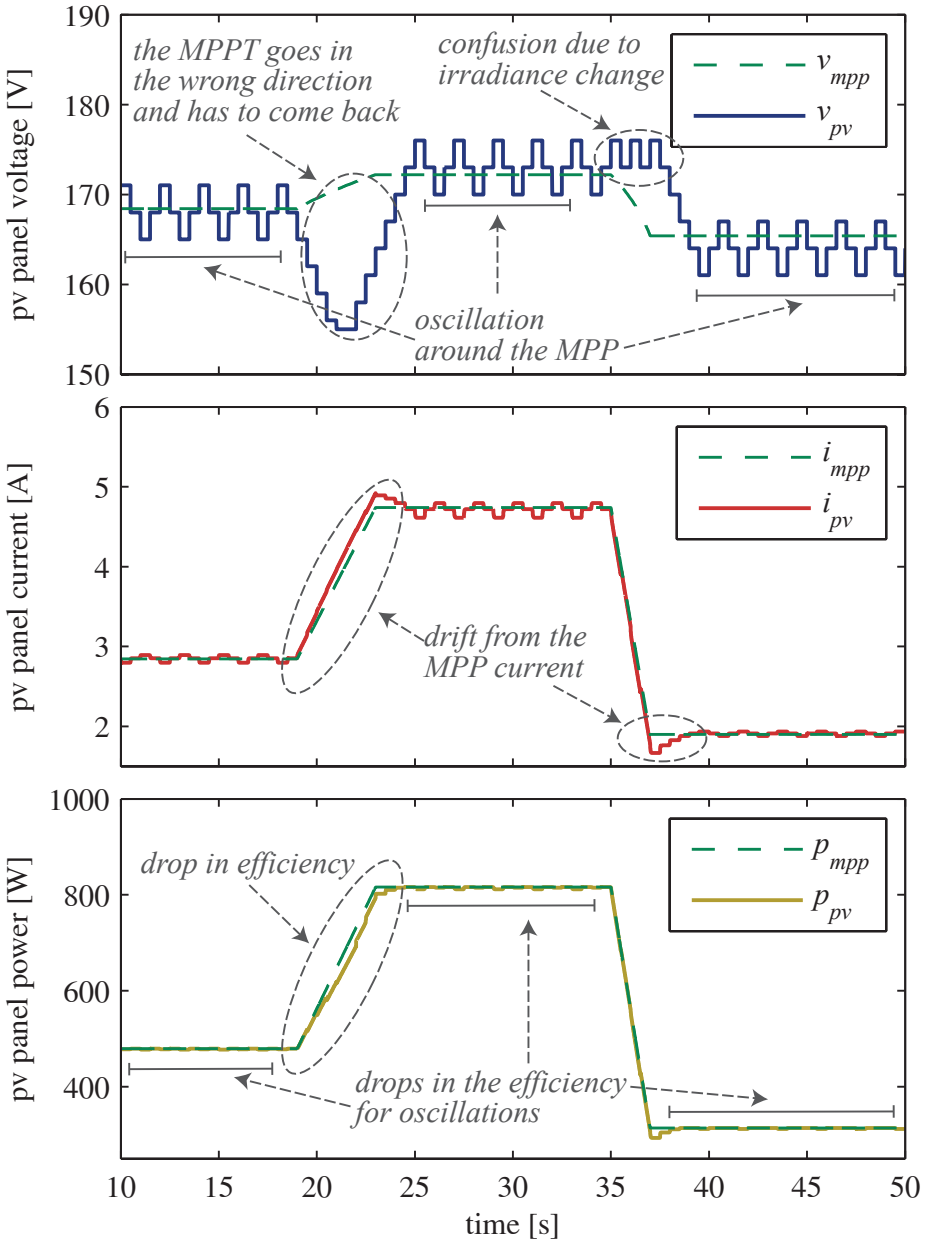

Figure 4.3: Standard P&O issues when the irradiation (G) slope starts during a falling step of the algorithm for v_{pv}, i_{pv} and p_{pv}.

The PV panel is configured to have 200 V open-circuit voltage and 5 A short-circuit current, with a Fill Factor (FF) of 0.8 at standard test conditions (STC, 1 kW/m^2 and 25 °C). The MPPTs are configured with the same voltage step for the P&O part and the same sampling period. The sampling period of the MPPT is established in 0.5 s and the

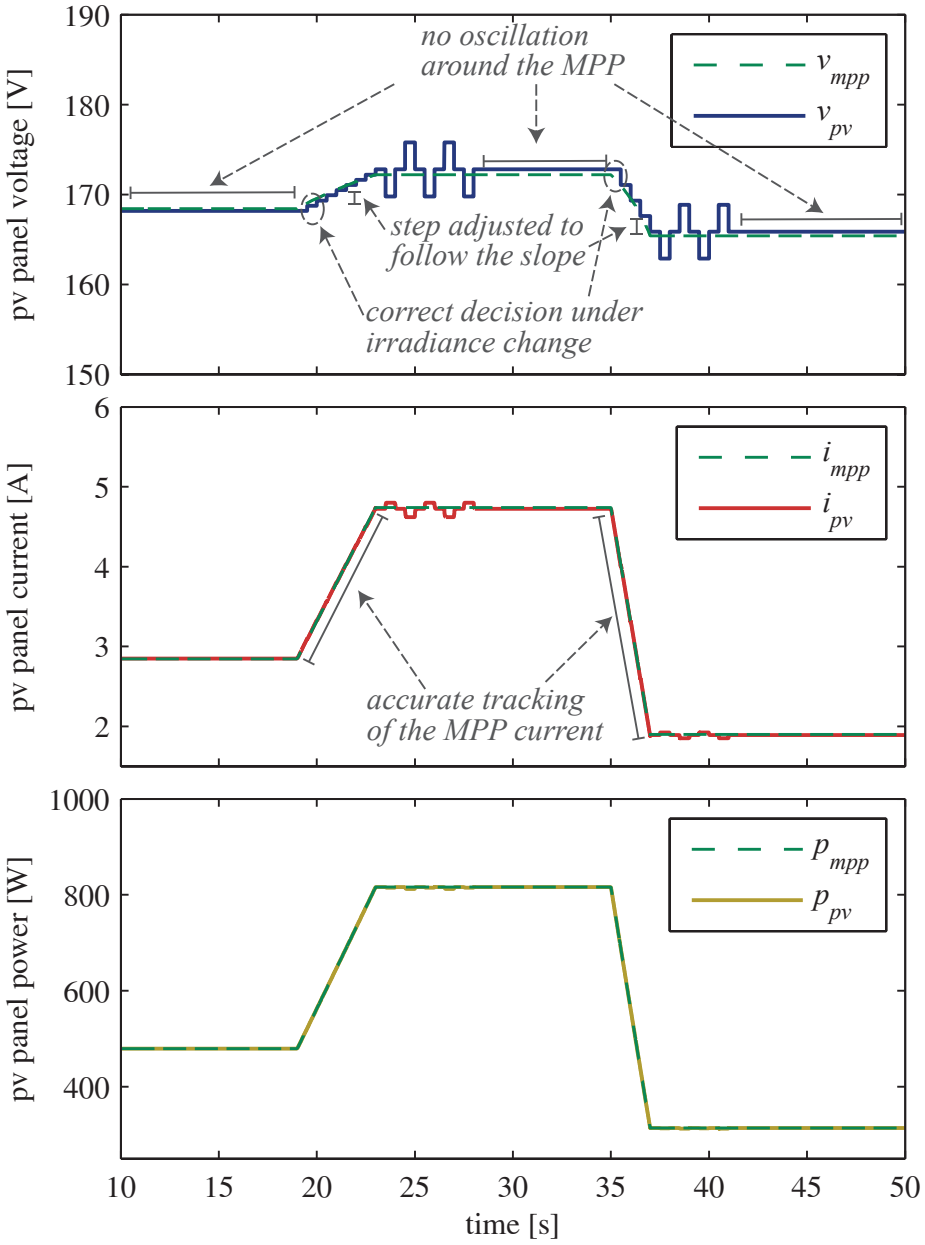

Figure 4.4: ZA-P&O MPPT strategy improvements in steady state and transient for the voltage v_{pv}, i_{pv} and p_{pv}.

fixed voltage step is 3 V. The testing profile is presented in Fig. 4.1. G starts at 0.6 kW/m^2; at $t = 19$ s, it starts increasing with a slope of 0.1 kW/m^{2}s. When it reaches 1.0 kW/m^2, it stops and waits for 11 s and then it starts decreasing with a slope of 0.3 kW/m^{2}s until it reaches 0.4 kW/m^2. Then it remains constant until the end of the simulation. To illustrate

the error in tracking for the standard P&O, two cases were studied, a) slope was started during a falling edge and b) during a raising edge of the MPPT by introducing a small displacement in the profile. The input signals to the MPPT are v_{pv}, i_{pv} and the error of the PI controller as indicated in Fig. 2.1. When the standard P&O is tested, the error signal is not used as one of the inputs. For the simulations, the threshold level of the current and the error (i_{Th} and e_{Th}) are set to zero, since there is no noise in this environment.

The results of the simulation for the standard P&O are displayed in Figs. 4.2 and 4.3, while the results for the ZA-P&O MPPT are presented in Fig. 4.4. When the transient profile starts, the standard P&O keeps going in the direction in which it was going before G changed (since it detects an increase in power) even when this direction is incorrect. In Fig. 4.2 this direction is correct, however, the tracking is not accurate since it is not able to detect that it is leaving the MPP voltage behind. Fig. 4.3 is an example of a bad decision: even when the tracking step is given in the incorrect direction, the MPPT algorithm keeps going in the same direction until it reaches the minimum operating voltage and has to return. When the irradiance decreases, it starts toggling in the same position, since any step produces a decrement in power. This deviation from the correct direction leads performance losses, since real profiles can have slopes for extended periods of time. Moreover, the standard MPPT algorithm is unable to adjust the tracking step to different δG; this leads to an algorithm that, even when it goes in the correct direction, may drift from the MPP because of the wrong step selection. This issue is shown in Fig. 4.2 where the operating point is increased until the drop is very large and it has to return.

The ZA-P&O MPPT strategy resolves those issues effectively as can be seen in Fig. 4.4. The idle operating mode allows the PV panel to operate in a smooth way when there is no need to keep tracking. When a change occurs in G, the strategy clearly identifies the correct direction to move the operating point and adjusts the step-size to provide a close

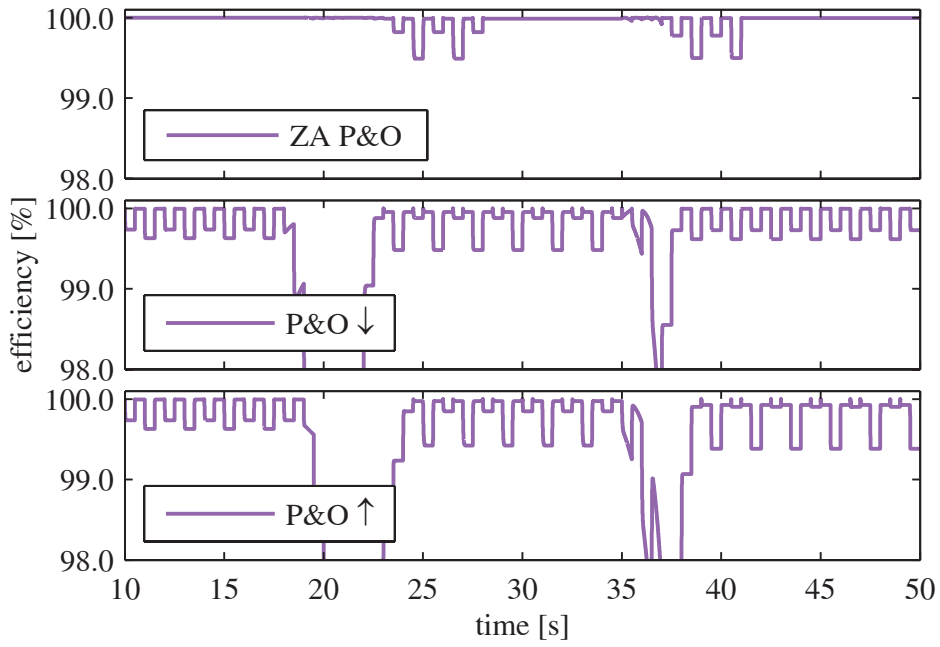

Figure 4.5: Efficiency of the PV panel for the ZA-P&O and the standard P&O when the slope starts in the falling edge (P&O ↓) and in the raising edge (P&O ↑).

tracking of the MPP. The effectiveness of the identification does not depend on the moment the irradiance slope starts.

The efficiency of the tracking for the three cases is shown in Fig. 4.5. It is evident that the ZA-P&O improves the overall performance: 1) in steady-state, the efficiency remains constant and close to 100% instead of oscillating periodically, 2) the correct direction is determined and 3) the step is adjusted; thus the efficiency remains high even during the transient, whereas the standard P&O leads to drops in efficiency.

Lastly, the transient trajectory is picture in the I-V plane in Fig. 4.6. This shows the trajectory of the tracking process for the P&O and for the ZA-P&O. The P&O deviates from the optimal trajectory, while the proposed strategy keeps very close track of it.

The experimental validation of the proposed strategy is presented in the next chapter. Using a similar profile, the promising results of the simulations will be tested.

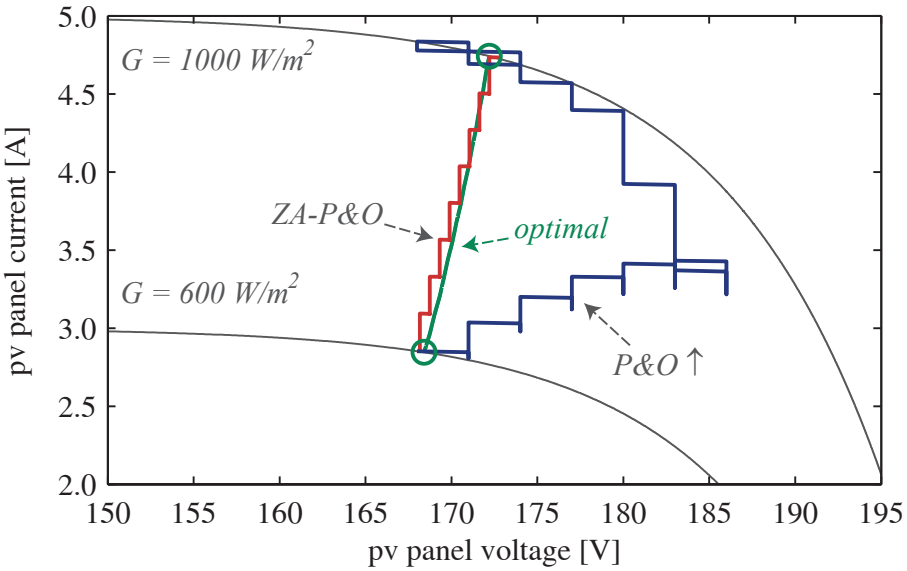

Figure 4.6: P&O undesirable drifting behavior versus ZA-P&O direct trajectory in the V-I plane. The proposed strategy closely follows the locus of MPP.

Chapter 5

Experimental Results

The simulation results in the previous chapter showed how the standard P&O algorithm has issues in steady state and while tracking changing environmental conditions and how the ZA-P&O MPPT mitigates the problem by using an indirect estimation of change in G. To further validate the algorithm, an experimental set-up was developed and the same algorithms were tested using the same irradiance profile. Additional validation of the characteristic features are presented using other profiles of G. These additional profiles include steeper and gradual ramps in G both decreasing and increasing from the initial state. This validation show how the adaptation of the step size provides accurate tracking of the MPP.

The experimental setup of Fig. 5.1 was developed with the same parameters than the simulation to validate the ZA-P&O MPPT strategy. The prototype was implemented using

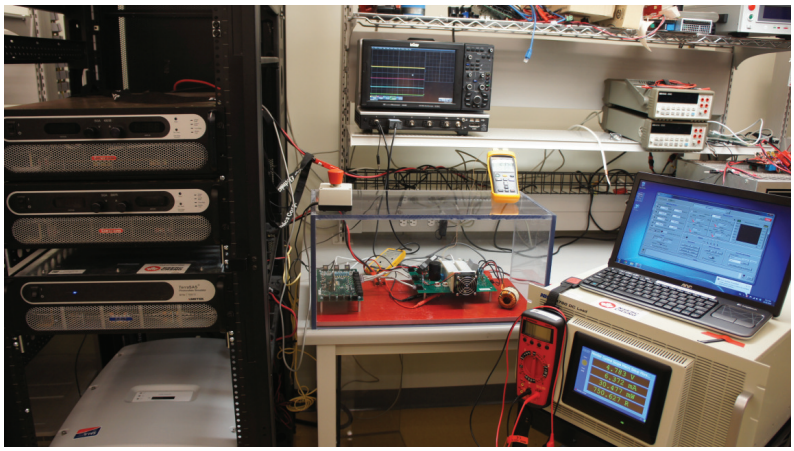

Figure 5.1: Picture of the experimental set-up.

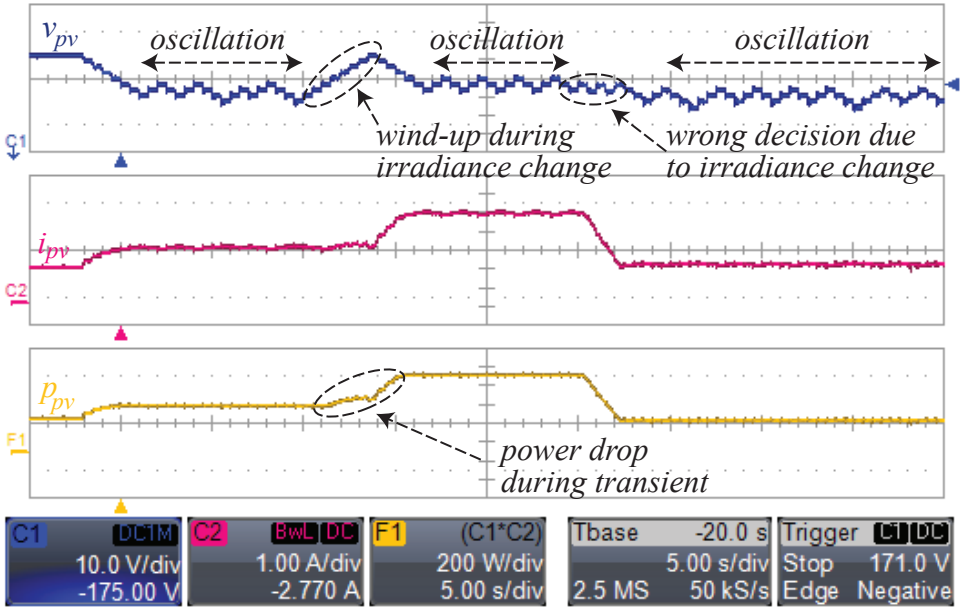

Figure 5.2: Standard P&O experimental capture when the irradiance transient starts in a raising edge of the MPPT showing the issues of steady state oscillations and inaccurate tracking of transients.

an industry-standard microcontroller (TI C2000 core) typically employed to control power converters. The experimental results are shown in Figs. 5.2 and 5.3 for the standard P&O when the slope starts at a falling edge and a raising edge respectively and in Fig. 5.4 for the proposed strategy. The experimental captures closely match the simulation results. The experimental captures for the standard P&O (Figs. 5.2 and 5.3) show the characteristic issues: oscillation in steady state, wrong direction and wind-up. The benefits of the ZA-P&O are clearly shown in Fig. 5.4, when compared with the standard P&O. The oscillation is removed and the step is given in the correct direction and magnitude, as shown in the fast re-establishment of the idle mode after the irradiance slope ends. Calculating the total power produced during the transient for the three cases shows that the ZA-P&O produces 0.4% more energy comparing Fig. 5.4 and 5.3 and 0.7% more energy comparing Fig. 5.4 and 5.2. The overall efficiency of the ZA-P&O MPPT for this transients is 99.3%.

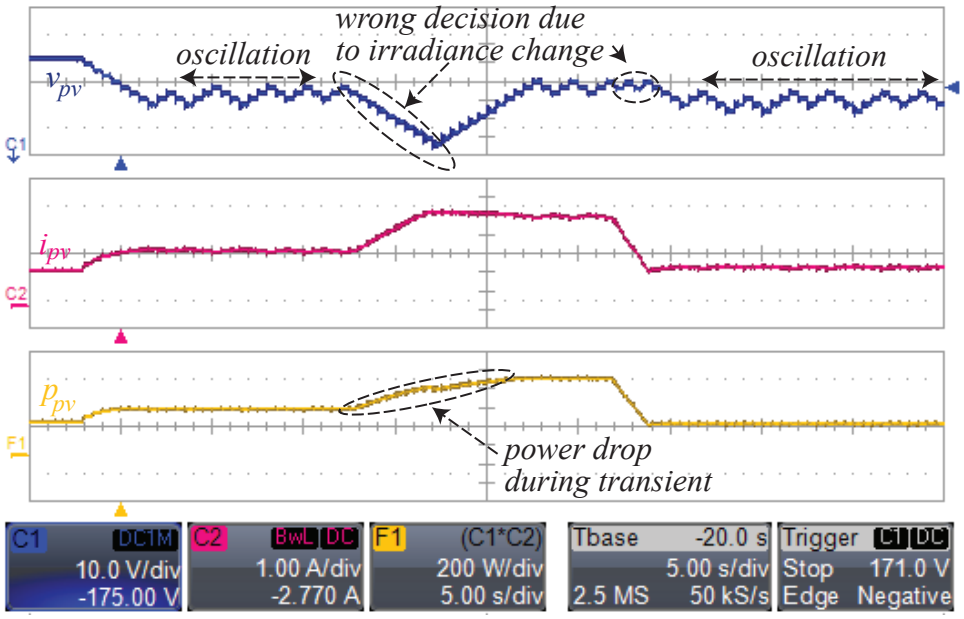

Figure 5.3: Standard P&O experimental capture when the irradiance transient starts in a falling edge of the MPPT showing the issues of steady state oscillations and inaccurate tracking of transients.

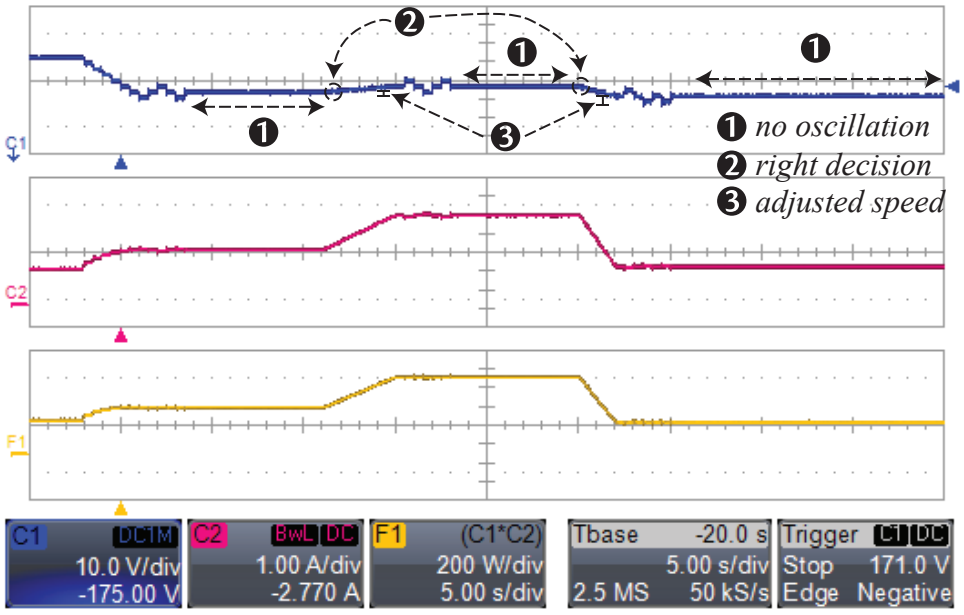

Figure 5.4: ZA-P&O experimental test; the improvements are shown with the steady state operation and the accurate and fast tracking during transients.

It can be seen in the experimental Figs. 5.2 and 5.3 that the standard P&O strategy drifts away from the MPP when G changes with a slope δG. Keeping the oscillation around the MPP in the idle condition increases the probability of making a mistake due to the noise in the measurement. This is demonstrated in Fig. 5.3, where the P&O process reaches the MPP during the first stage and works with three levels but suddenly drifts away and returns. The ZA-P&O MPPT strategy benefits from the removal of this perturbation to enable a clearer measure of the change in G, which is represented by ❷ in Fig. 5.4. The use of an indirect estimation though the control loop allows this estimation to be done without increasing the complexity of the system, since the signals are already available inside the micorcontroller.

In order to test the irradiance slope identification and multi-level step-size adaptation, two different profiles are introduced and tested in the experimental set-up. The profile in Fig. 5.5 shows the PV panel operating at 1.0 $\mathrm{kWm^{-2}}$ followed by a gradual drop in irradiance during 5 s period of time. After staying at 0.5 $\mathrm{kWm^{-2}}$ during 5 s the profile returns to 1.0 $\mathrm{kWm^{-2}}$ in 1 s. The profile in Fig. 5.6 a reflected version of the previous one, starting at low irradiance and gradually reaching the 1.0 $\mathrm{kWm^{-2}}$ level. Using this profile it is possible to test the ZA-P&O algorithm for a range of slopes both positive and negative showing the step size adaptation feature.

The captures in Fig. 5.7 and Fig. 5.8 show the ZA-P&O MPPT for the different G-profiles stated before. The captures show details of the behavior under this changing environmental conditions, with a closer time scale and vertical scales compared with the one in Fig. 5.4. The experimental set shows how the ZA-P&O reacts to a very fast transient and a very slow one. As can be seen, the estimation of the new position ensures the correct direction and places the operating point close to the MPP in such a way that the local optimizations (activated

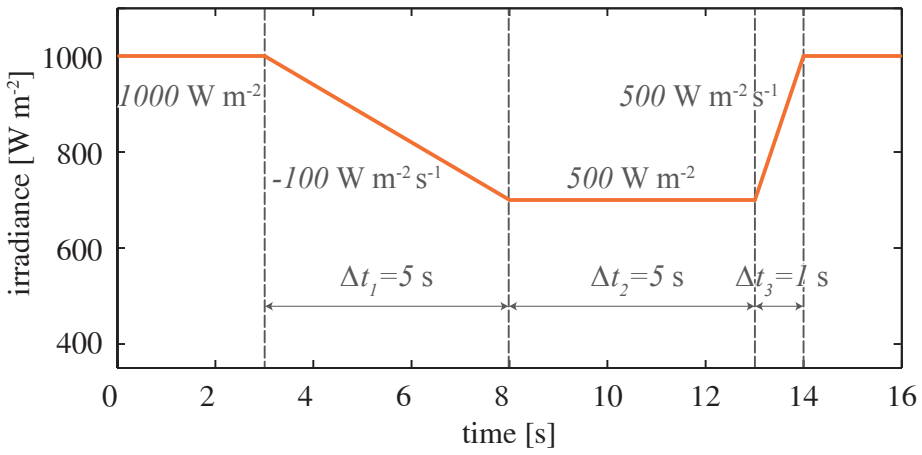

Figure 5.5: Irradiance profile to test the adaptive step feature of the ZA-P&O MPPT strategy. A gradual transition from a high-irradiance level to a low-irradiance level followed by a fast return is implemented.

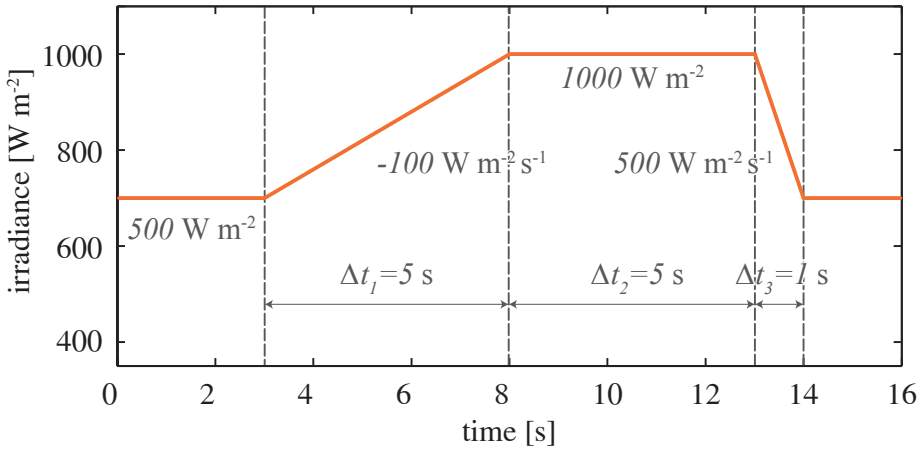

Figure 5.6: Irradiance profile to test the adaptive step feature of the ZA-P&O MPPT strategy. A gradual transition from a low-irradiance level to a high-irradiance level followed by a fast return is implemented.

after the transient) can locate the MPP in a few cycles and reactivate the Idle mode reducing the losses to a minimum.

The ZA-P&O was tested against the standard P&O algorithm in an experimental set-up using the same profile of G than the simulations and obtaining equivalent results. Additional profiles were tested in order to further validate the adaptive-step feature of the proposed

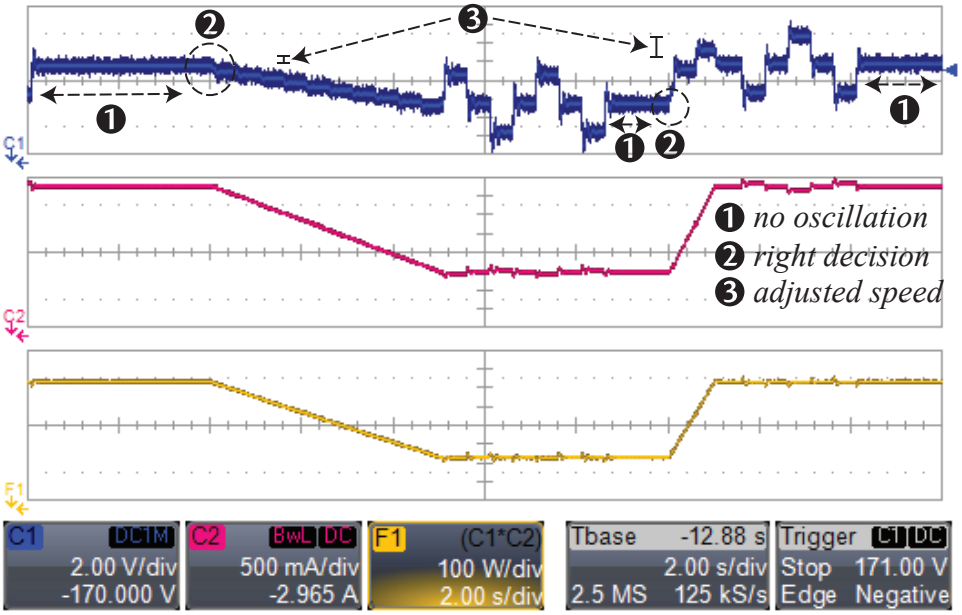

Figure 5.7: ZA-P&O experimental test for a step-down change from 1 kW m^{-2} to 500 W m^{-2} in 5 s and then back to 1 kW m^{-2} in 1 s.

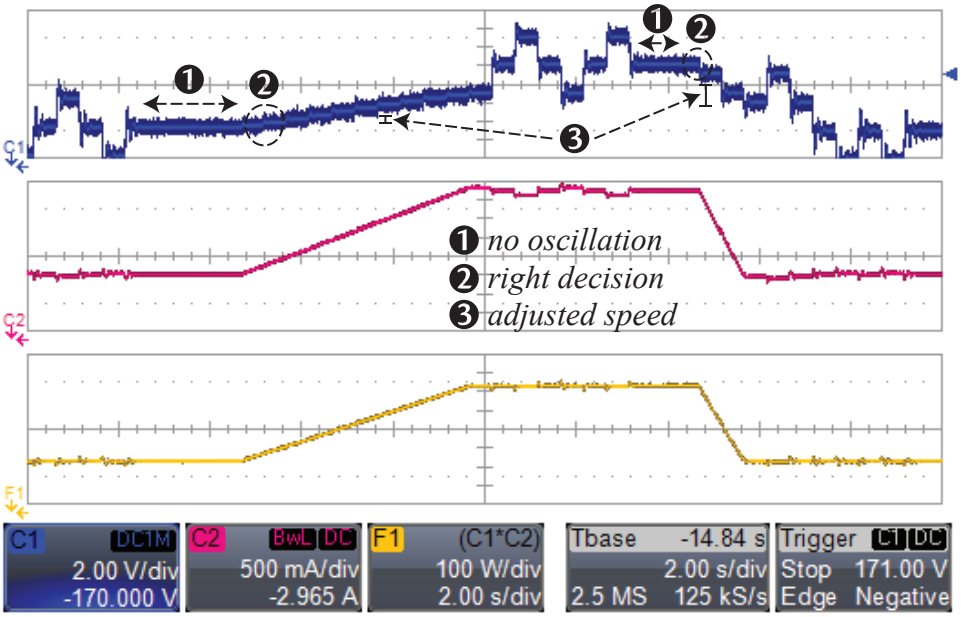

Figure 5.8: ZA-P&O experimental test for a step-up change from 500 W m^{-2} to 100 W m^{-2} in 5 s and then back to 500 W m^{-2} in 1 s.

strategy. The captures show the indirect identification of the change G allows the MPPT algorithm to avoid making mistakes and tracking in the correct direction even with different

slopes. Besides the increment in extracted energy, the ZA-P&O creates a cleaner operating condition for the converter with no unnecessary oscillations and long tracking transients. The addition of these features creates a more reliable MPPT algorithm when compared with the P&O and allow for more energy to be harvested from the solar panel.

Chapter 6

Conclusions

6.1 Summary

Photovoltaic (PV) energy systems use power electronics converters to interface the energy source with either the load or the grid. This is done in order to modify the characteristics of the voltage/current extracted from the PV panel to match the needs of the load and to adapt the impedance connected to the panel to extract the maximum power. This is called Maximum Power Point Tracking (MPPT). In the industry, the standard MPPT algorithm is the Perturb and Observe (P&O) or the incremental conductance (InCond). Both of them are based on the hill-climbing method and have the same issues that introduce losses: oscillations in steady-state, errors during changing environmental conditions and inability to detect the rate of change of the irradiance and adjust the step-size to accurately track it.

This thesis introduced the Zero-oscillation, Adaptive-step Perturb and Observe (ZA-P&O) MPPT strategy for PV panels. This combined strategy reduced steady-state losses and improved transient behavior during slope changes irradiance, while maintaining a similar implementation complexity compared with industry-standard algorithms. The enhanced behavior resulted from the combination of three techniques: 1) idle operation when steady-state is reached, 2) correct irradiance change identification and 3) multi-level adaptive tracking step. The idle operation was possible due to the identification of the irradiance slope through a current monitoring algorithm. The adaptive tracking speed minimized error during a fast change in irradiance.

The proposed combined techniques were studied with simulations and validated through experimental results implemented in a low cost microcontroller. The overall performance improvements, both in steady-state and with different irradiance change profiles show the benefits of the combined techniques.

The contribution investigated in this thesis has been published IEEE PEDG 2013 [1] and IEEE Transactions on Industrial Electronics [2].

6.2 Future Work

The algorithm developed in this work provides an original contribution to the field of MPPT for photovoltaic applications. The extension of this concept to other renewable and alternative energy sources (wind, hydro, fuel cells, etc.) is being studied and a research paper is being prepared. A research paper involving advanced control strategies for power converters involved in MPPT for PV applications was accepted for PEDG 2014. A research paper on high speed MPPT strategies for electric vehicles is under development.

The use of indirect environmental changes identification to improve the MPPT capabilities of the converter presents a useful tool for all renewable energy sources in the future.

Bibliography

[1] F. Paz and M. Ordonez, "Zero-oscillation adaptive-step solar maximum power point tracking for rapid irradiance tracking and steady-state losses minimization," in *IEEE Int. Symp. Power Electronics for Distributed Generation Systems (PEDG)*, Rorgers, AR, Jul. 2013, pp. 1–6, © 2013 IEEE.

[2] F. Paz and M. Ordonez, "Zero oscillation and irradiance slope tracking for photovoltaic mppt," *IEEE Trans. Ind. Electron.*, vol. 61, no. 11, pp. 6138 – 6147, Nov. 2014, © 2014 IEEE.

[3] "Photovoltaics report," FRAUNHOFER INSTITUTE FOR SOLAR ENERGY SYSTEMS ISE, Tech. Rep., Nov. 2013. [Online]. Available: www.ise.fraunhofer.de

[4] G. Hart, H. Branz, and C. C. III, "Experimental tests of open-loop maximum-power-point tracking techniques for photovoltaic arrays," *Solar Cells*, vol. 13, no. 2, pp. 185 – 195, 1984.

[5] J. Applebaum, "The quality of load matching in a direct-coupling photovoltaic system," *IEEE Trans. Energy Convers.*, vol. EC-2, no. 4, pp. 534–541, Dec 1987.

[6] J. Dunlop, "Analysis and design optimization of photovoltaic water pumping systems," in *IEEE Photovoltaic Specialists Conf. (PVSC)*, Las Vegas (NV), Sep. 1988, pp. 1182–1187 vol.2.

[7] J. Appelbaum and M. Sarma, "The operation of permanent magnet dc motors powered by a common source of solar cells," *IEEE Trans. Energy Convers.*, vol. 4, no. 4, pp. 635–642, Dec 1989.

[8] J. Appelbaum and S. Singer, "Magnification of starting torques of dc motors by maximum power point trackers in photovoltaic systems," in *Intersociety Energy Conversion Engineering Conference (IECEC)*, Aug. 1989, pp. 749–754 vol.2.

[9] J. Appelbaum, "The operation of loads powered by separate sources or by a common source of solar cells," *IEEE Trans. Energy Convers.*, vol. 4, no. 3, pp. 351–357, Sep. 1989.

[10] J. H. R. Enslin, "Maximum power point tracking: a cost saving necessity in solar energy systems," in *IEEE Annu. Conf. Industrial Electronics (IECON)*, Nov. 1990, pp. 1073–1077 vol.2.

[11] A. Pandey, N. Dasgupta, and A. Mukerjee, "A simple single-sensor mppt solution," *IEEE Trans. Power Electron.*, vol. 22, no. 2, pp. 698–700, Mar. 2007.

[12] D. Patterson, "Electrical system design for a solar powered vehicle," in *IEEE Annu. Power Electronics Specialists Conf. (PESC)*, Jan. 1990, pp. 618–622.

[13] W. Li, Y. Zheng, W. Li, Y. Zhao, and X. He, "A smart and simple pv charger for portable applications," in *IEEE Annu. Applied Power Electronics Conf. and Expo. (APEC)*, Feb. 2010, pp. 2080–2084.

[14] M. Masoum, H. Dehbonei, and E. Fuchs, "Theoretical and experimental analyses of photovoltaic systems with voltageand current-based maximum power-point tracking," *IEEE Trans. Energy Convers.*, vol. 17, no. 4, pp. 514 – 522, Dec. 2002.

[15] J. Appelbaum, "Discussion of "theoretical and experimental analyses of photovoltaic systems with voltage and current-based maximum power point tracking"," *IEEE Trans. Energy Convers.*, vol. 19, no. 3, pp. 651–652, Sep. 2004.

[16] J. Martynaitis, "Discussion of "theoretical and experimental analyses of photovoltaic systems with voltage and current-based maximum power point tracking"," *IEEE Trans. Energy Convers.*, vol. 19, no. 3, pp. 652–, Sep. 2004.

[17] M. Masoum, H. Dehbonei, and E. Fuchs, "Closure on "theoretical and experimental analyses of photovoltaic systems with voltage and current-based maximum power point tracking"," *IEEE Trans. Energy Convers.*, vol. 19, no. 3, pp. 652–653, Sep. 2004.

[18] A. Murtaza, H. Sher, M. Chiaberge, D. Boero, M. De Giuseppe, and K. Addoweesh, "Comparative analysis of maximum power point tracking techniques for pv applications," in *Int. Multi Topic Conference (INMIC)*, Dec 2013, pp. 83–88.

[19] B. Subudhi and R. Pradhan, "A comparative study on maximum power point tracking techniques for photovoltaic power systems," *IEEE Trans. Sustain. Energy*, vol. 4, no. 1, pp. 89 –98, Jan. 2013.

[20] O. Lopez-Lapena, M. Penella, and M. Gasulla, "A closed-loop maximum power point tracker for subwatt photovoltaic panels," *IEEE Trans. Ind. Electron.*, vol. 59, no. 3, pp. 1588–1596, Mar. 2012.

[21] A. Weddell, G. Merrett, and B. Al-Hashimi, "Photovoltaic sample-and-hold circuit enabling mppt indoors for low-power systems," *IEEE Trans. Circuits Syst. I, Reg. Papers*, vol. 59, no. 6, pp. 1196 –1204, Jun. 2012.

[22] S. Kjaer, "Evaluation of the "hill climbing" and the "incremental conductance" maximum power point trackers for photovoltaic power systems," *IEEE Trans. Energy Convers.*, vol. 27, no. 4, pp. 922 –929, Dec. 2012.

[23] G. Petrone, G. Spagnuolo, R. Teodorescu, M. Veerachary, and M. Vitelli, "Reliability issues in photovoltaic power processing systems," *IEEE Trans. Ind. Electron.*, vol. 55, no. 7, pp. 2569–2580, Jul. 2008.

[24] E. Roman, R. Alonso, P. Ibanez, S. Elorduizapatarietxe, and D. Goitia, "Intelligent pv module for grid-connected pv systems," *IEEE Trans. Ind. Electron.*, vol. 53, no. 4, pp. 1066–1073, Jun. 2006.

[25] A. Ridge and G. Amaratunga, "Photovoltaic maximum power point tracking for mobile applications," *Electronics Letters*, vol. 46, no. 22, pp. 1520–1521, Oct. 2010.

[26] A. Safari and S. Mekhilef, "Simulation and hardware implementation of incremental conductance mppt with direct control method using cuk converter," *IEEE Trans. Ind. Electron.*, vol. 58, no. 4, pp. 1154–1161, Apr. 2011.

[27] D. Sera, L. Mathe, T. Kerekes, S. Spataru, and R. Teodorescu, "On the perturb-and-observe and incremental conductance mppt methods for pv systems," *IEEE J. Photovolt.*, vol. 3, no. 3, pp. 1070–1078, Jul. 2013.

[28] M. Elgendy, B. Zahawi, and D. Atkinson, "Assessment of the incremental conductance maximum power point tracking algorithm," *IEEE Trans. Sustain. Energy*, vol. 4, no. 1, pp. 108 –117, Jan. 2013.

[29] N. Femia, G. Petrone, G. Spagnuolo, and M. Vitelli, "Optimization of perturb and observe maximum power point tracking method," *IEEE Trans. Power Electron.*, vol. 20, no. 4, pp. 963 – 973, Jul. 2005.

[30] N. Femia, G. Petrone, G. Spagnuolo, and M. Vitelli, "A technique for improving p&o mppt performances of double-stage grid-connected photovoltaic systems," *IEEE Trans. Ind. Electron.*, vol. 56, no. 11, pp. 4473–4482, Nov. 2009.

[31] M. Elgendy, B. Zahawi, and D. Atkinson, "Assessment of perturb and observe mppt algorithm implementation techniques for pv pumping applications," *IEEE Trans. Sustain. Energy*, vol. 3, no. 1, pp. 21 –33, Jan. 2012.

[32] M. de Brito, L. Galotto, L. Sampaio, G. de Azevedo e Melo, and C. Canesin, "Evaluation of the main mppt techniques for photovoltaic applications," *IEEE Trans. Ind. Electron.*, vol. 60, no. 3, pp. 1156 –1167, Mar. 2013.

[33] C. Sullivan, J. Awerbuch, and A. Latham, "Decrease in photovoltaic power output from ripple: Simple general calculation and the effect of partial shading," *IEEE Trans. Power Electron.*, vol. 28, no. 2, pp. 740 –747, Feb. 2013.

[34] R. Faranda, S. Leva, and V. Maugeri, "Mppt techniques for pv systems: Energetic and cost comparison," in *IEEE Power and Energy Society General Meeting*, Pitsburg, PA, Jul. 2008, pp. 1–6.

[35] M. Berrera, A. Dolara, R. Faranda, and S. Leva, "Experimental test of seven widely-adopted mppt algorithms," in *IEEE Bucharest PowerTech (BPT)*, Bucharest, Romania, Jun. 2009, pp. 1–8.

[36] A. Abdelsalam, A. Massoud, S. Ahmed, and P. Enjeti, "High-performance adaptive perturb and observe mppt technique for photovoltaic-based microgrids," *IEEE Trans. Power Electron.*, vol. 26, no. 4, pp. 1010–1021, Apr. 2011.

[37] N. Khaehintung, T. Wiangtong, and P. Sirisuk, "Fpga implementation of mppt using variable step-size p o algorithm for pv applications," in *Int. Symp. Communications and Information Technologies (ISCIT)*, Oct. 2006, pp. 212–215.

[38] M. Mohd Zainuri, M. Mohd Radzi, A. Soh, and N. Rahim, "Development of adaptive perturb and observe-fuzzy control maximum power point tracking for photovoltaic boost dc-dc converter," *IET Renew. Power Gen.*, vol. 8, no. 2, pp. 183–194, Mar. 2014.

[39] S. Kollimalla and M. Mishra, "Variable perturbation size adaptive p amp;o mppt algorithm for sudden changes in irradiance," *IEEE Trans. Sustain. Energy*, vol. 5, no. 3, pp. 718–728, Jul. 2014.

[40] W. Xiao and W. Dunford, "A modified adaptive hill climbing mppt method for photovoltaic power systems," in *IEEE Annu. Power Electronics Specialists Conf. (PESC)*, vol. 3, Aachen, Germany, Jun. 2004, pp. 1957 – 1963 Vol.3.

[41] F. Liu, S. Duan, F. Liu, B. Liu, and Y. Kang, "A variable step size inc mppt method for pv systems," *IEEE Trans. Ind. Electron.*, vol. 55, no. 7, pp. 2622–2628, Jul. 2008.

[42] Q. Mei, M. Shan, L. Liu, and J. Guerrero, "A novel improved variable step-size incremental-resistance mppt method for pv systems," *IEEE Trans. Ind. Electron.*, vol. 58, no. 6, pp. 2427 –2434, Jun. 2011.

[43] H. Koizumi and K. Kurokawa, "Plane division maximum power point tracking method for pv module integrated converter," in *IEEE Int. Symp. Industrial Electronics (ISIE)*, vol. 2, Quebec, Canada, Jul. 2006, pp. 1265–1270.

[44] H. Koizumi, "A summary of plane division maximum power point tracking methods," in *IEEE Int. Conf. on Sustainable Energy Technologies (ICSET)*, Singapore, Singapore, Nov. 2008, pp. 306–311.

[45] H. Patel and V. Agarwal, "Maximum power point tracking scheme for pv systems operating under partially shaded conditions," *IEEE Trans. Ind. Electron.*, vol. 55, no. 4, pp. 1689–1698, Apr. 2008.

[46] A. Zbeeb, V. Devabhaktuni, and A. Sebak, "Improved photovoltaic mppt algorithm adapted for unstable atmospheric conditions and partial shading," in *Int. Conf. Clean Electrical Power*, Jun. 2009, pp. 320–323.

[47] E. Koutroulis and F. Blaabjerg, "A new technique for tracking the global maximum power point of pv arrays operating under partial-shading conditions," *IEEE J. Photovolt.*, vol. 2, no. 2, pp. 184–190, Apr. 2012.

[48] J. Bastidas-Rodriguez, E. Franco, G. Petrone, C. Ramos-Paja, and G. Spagnuolo, "Maximum power point tracking architectures for photovoltaic systems in mismatching conditions: a review," *IET Power Electron.*, vol. 7, no. 6, pp. 1396–1413, Jun. 2014.

[49] K. Chen, S. Tian, Y. Cheng, and L. Bai, "An improved mppt controller for photovoltaic system under partial shading condition," *IEEE Trans. Sustain. Energy*, vol. 5, no. 3, pp. 978–985, Jul. 2014.

[50] K. S. Tey and S. Mekhilef, "Modified incremental conductance algorithm for photovoltaic system under partial shading conditions and load variation," *IEEE Trans. Ind. Electron.*, vol. 61, no. 10, pp. 5384–5392, Oct. 2014.

[51] D. Sera, R. Teodorescu, J. Hantschel, and M. Knoll, "Optimized maximum power point tracker for fast-changing environmental conditions," *IEEE Trans. Ind. Electron.*, vol. 55, no. 7, pp. 2629 –2637, Jul. 2008.

[52] R. Kadri, J.-P. Gaubert, and G. Champenois, "An improved maximum power point tracking for photovoltaic grid-connected inverter based on voltage-oriented control," *IEEE Trans. Ind. Electron.*, vol. 58, no. 1, pp. 66 –75, Jan. 2011.

[53] P. Midya, P. Krein, R. Turnbull, R. Reppa, and J. Kimball, "Dynamic maximum power point tracker for photovoltaic applications," in *IEEE Annu. Power Electronics Specialists Conf. (PESC)*, vol. 2, Jun. 1996, pp. 1710–1716 vol.2.

[54] T. Esram, J. Kimball, P. Krein, P. Chapman, and P. Midya, "Dynamic maximum power point tracking of photovoltaic arrays using ripple correlation control," *IEEE Trans. Power Electron.*, vol. 21, no. 5, pp. 1282–1291, Sep. 2006.

[55] S. Jain and V. Agarwal, "Comparison of the performance of maximum power point tracking schemes applied to single-stage grid-connected photovoltaic systems," *Electric Power Applications, IET*, vol. 1, no. 5, pp. 753–762, Sep. 2007.

[56] J. Kimball and P. Krein, "Discrete-time ripple correlation control for maximum power point tracking," *IEEE Trans. Power Electron.*, vol. 23, no. 5, pp. 2353–2362, Sep. 2008.

[57] A. Bazzi and P. Krein, "Concerning maximum power point tracking for photovoltaic optimization using ripple-based extremum seeking control," *IEEE Trans. Power Electron.*, vol. 26, no. 6, pp. 1611–1612, Jun. 2011.

[58] R. Khanna, Q. Zhang, W. Stanchina, G. Reed, and Z.-H. Mao, "Maximum power point tracking using model reference adaptive control," *IEEE Trans. Power Electron.*, vol. 29, no. 3, pp. 1490–1499, Mar. 2014.

[59] J. Blanes, F. Toledo, S. Montero, and A. Garrigos, "In-site real-time photovoltaic i-v curves and maximum power point estimator," *IEEE Trans. Power Electron.*, vol. 28, no. 3, pp. 1234 –1240, Mar. 2013.

[60] T. Esram and P. Chapman, "Comparison of photovoltaic array maximum power point tracking techniques," *IEEE Trans. Energy Convers.*, vol. 22, no. 2, pp. 439–449, Jun. 2007.

[61] N. Mutoh, M. Ohno, and T. Inoue, "A method for mppt control while searching for parameters corresponding to weather conditions for pv generation systems," *IEEE Trans. Ind. Electron.*, vol. 53, no. 4, pp. 1055 –1065, Jun. 2006.

[62] L. Cristaldi, M. Faifer, M. Rossi, and S. Toscani, "An improved model-based maximum power point tracker for photovoltaic panels," *IEEE Trans. Instrum. Meas.*, vol. 63, no. 1, pp. 63–71, Jan. 2014.

[63] X. Li, Y. Li, and J. Seem, "Maximum power point tracking for photovoltaic system using adaptive extremum seeking control," *IEEE Trans. Control Syst. Technol.*, vol. 21, no. 6, pp. 2315–2322, Nov. 2013.

[64] W.-M. Lin, C.-M. Hong, and C.-H. Chen, "Neural-network-based mppt control of a stand-alone hybrid power generation system," *IEEE Trans. Power Electron.*, vol. 26, no. 12, pp. 3571–3581, Dec 2011.

[65] L. Elobaid, A. Abdelsalam, and E. Zakzouk, "Artificial neural network based maximum power point tracking technique for pv systems," in *IEEE Annu. Conf. Industrial Electronics (IECON)*, Montreal, QC, Oct. 2012, pp. 937–942.

[66] M. Veerachary, T. Senjyu, and K. Uezato, "Neural-network-based maximum-power-point tracking of coupled-inductor interleaved-boost-converter-supplied pv system using fuzzy controller," *IEEE Trans. Ind. Electron.*, vol. 50, no. 4, pp. 749–758, Aug. 2003.

[67] Syafaruddin, E. Karatepe, and T. Hiyama, "Artificial neural network-polar coordinated fuzzy controller based maximum power point tracking control under partially shaded conditions," *IET Renew. Power Gen.*, vol. 3, no. 2, pp. 239–253, Jun. 2009.

[68] A. Al Nabulsi and R. Dhaouadi, "Efficiency optimization of a dsp-based standalone pv system using fuzzy logic and dual-mppt control," *IEEE Trans. Ind. Electron.*, vol. 8, no. 3, pp. 573 –584, Aug. 2012.

[69] C.-U. Lee, J.-S. Ko, T.-Y. Seo, D.-K. Kim, and D.-H. Chung, "The mppt control of photovoltaic system using fuzzy-pi controller," in *Int. Conf. Electrical Machines and Systems (ICEMS)*, Oct. 2013, pp. 303–305.

[70] C.-S. Chiu, "T-s fuzzy maximum power point tracking control of solar power generation systems," *IEEE Trans. Energy Convers.*, vol. 25, no. 4, pp. 1123–1132, Dec 2010.

[71] C.-S. Chiu and Y.-L. Ouyang, "Robust maximum power tracking control of uncertain photovoltaic systems: A unified t-s fuzzy model-based approach," *IEEE Trans. Control Syst. Technol.*, vol. 19, no. 6, pp. 1516–1526, Nov. 2011.

[72] B. Alajmi, K. Ahmed, S. Finney, and B. Williams, "A maximum power point tracking technique for partially shaded photovoltaic systems in microgrids," *IEEE Trans. Ind. Electron.*, vol. 60, no. 4, pp. 1596 –1606, Apr. 2013.

[73] Y. Hu, J. Liu, and B. Liu, "A mppt control method of pv system based on fuzzy logic and particle swarm optimization," in *Int. Conf. Intelligent System Design and Engineering Application (ISDEA)*, Jan. 2012, pp. 73–75.

[74] Y. Liu, D. Xia, and Z. He, "Mppt of a pv system based on the particle swarm optimization," in *Int. Conf. Electric Utility Deregulation and Restructuring and Power Technologies (DRPT)*, Jul. 2011, pp. 1094–1096.

[75] M. Miyatake, M. Veerachary, F. Toriumi, N. Fujii, and H. Ko, "Maximum power point tracking of multiple photovoltaic arrays: A pso approach," *IEEE Trans. Aerosp. Electron. Syst.*, vol. 47, no. 1, pp. 367–380, Jan. 2011.

[76] M. Abdullah, A. Yatim, C. Tan, and A. Samosir, "Particle swarm optimization-based maximum power point tracking algorithm for wind energy conversion system," in *IEEE Int. Conf. on Power and Energy (PECon)*, Dec 2012, pp. 65–70.

[77] K. Ishaque, Z. Salam, M. Amjad, and S. Mekhilef, "An improved particle swarm optimization (pso) and based mppt for pv with reduced steady-state oscillation," *IEEE Trans. Power Electron.*, vol. 27, no. 8, pp. 3627–3638, Aug. 2012.

[78] K. Ishaque and Z. Salam, "A deterministic particle swarm optimization maximum power point tracker for photovoltaic system under partial shading condition," *IEEE Trans. Ind. Electron.*, vol. 60, no. 8, pp. 3195–3206, Aug. 2013.

[79] A. Bidram, A. Davoudi, and R. Balog, "Control and circuit techniques to mitigate partial shading effects in photovoltaic arrays," *IEEE J. Photovolt.*, vol. 2, no. 4, pp. 532–546, Oct. 2012.

[80] F. Giraud and Z. Salameh, "Analysis of the effects of a passing cloud on a grid-interactive photovoltaic system with battery storage using neural networks," *IEEE Trans. Energy Convers.*, vol. 14, no. 4, pp. 1572–1577, Dec 1999.

[81] M. Boztepe, F. Guinjoan, G. Velasco-Quesada, S. Silvestre, A. Chouder, and E. Karatepe, "Global mppt scheme for photovoltaic string inverters based on restricted voltage window search algorithm," *IEEE Trans. Ind. Electron.*, vol. 61, no. 7, pp. 3302–3312, Jul. 2014.

[82] E. Mamarelis, G. Petrone, and G. Spagnuolo, "Design of a sliding-mode-controlled sepic for pv mppt applications," *IEEE Trans. Ind. Electron.*, vol. 61, no. 7, pp. 3387–3398, Jul. 2014.

[83] N. Femia, D. Granozio, G. Petrone, G. Spagnuolo, and M. Vitelli, "Optimized one-cycle control in photovoltaic grid connected applications," *IEEE Trans. Aerosp. Electron. Syst*, vol. 42, no. 3, pp. 954–972, Jul. 2006.

[84] M. Fortunato, A. Giustiniani, G. Petrone, G. Spagnuolo, and M. Vitelli, "Maximum power point tracking in a one-cycle-controlled single-stage photovoltaic inverter," *IEEE Trans. Ind. Electron.*, vol. 55, no. 7, pp. 2684–2693, Jul. 2008.

[85] E. Sreeraj, K. Chatterjee, and S. Bandyopadhyay, "One-cycle-controlled single-stage single-phase voltage-sensorless grid-connected pv system," *IEEE Trans. Ind. Electron.*, vol. 60, no. 3, pp. 1216–1224, Mar. 2013.

[86] A. Luque and S. Hegedus, *Handbook of Photovoltaic Science and Engineering.* Wiley, 2003.